WARWICK
THE UNIVERSITY OF WARWICK

Original citation:
Mu, Mulan, Wan, Chaoying and McNally, Tony. (2017) Thermal conductivity of 2D nano-structured graphitic materials and their composites with epoxy resins. 2D Materials, 4 (4). 042001.

Permanent WRAP URL:
http://wrap.warwick.ac.uk/89768

Copyright and reuse:
The Warwick Research Archive Portal (WRAP) makes this work of researchers of the University of Warwick available open access under the following conditions.

A note on versions:
The version presented in WRAP is the published version, or, version of record, and may be cited as it appears here.

For more information, please contact the WRAP Team at: wrap@warwick.ac.uk

warwick.ac.uk/lib-publications

Thermal conductivity of 2D nano-structured graphitic materials and their composites with epoxy resins

Mulan Mu, Chaoying Wan and Tony McNally*

International Institute for Nanocomposites Manufacturing (IINM), WMG, University of Warwick, UK, CV4 7AL

E-mail: t.mcnally@warwick.ac.uk

Abstract

The outstanding thermal conductivity (λ) of graphene and its derivatives offers a potential route to enhance the thermal conductivity of epoxy resins. Key challenges still need to be overcome to ensure effective dispersion and distribution of 2D graphitic fillers throughout the epoxy matrix. 2D filler type, morphology, surface chemistry and dimensions are all important factors in determining filler thermal conductivity and *de facto* the thermal conductivity of the composite material. To achieve significant enhancement in the thermal conductivity of epoxy composites, different strategies are required to minimise phonon scattering at the interface between the nano-filler and epoxy matrix, including chemical functionalisation of the filler surfaces such that interactions between filler and matrix are promoted and interfacial thermal resistance (ITR) reduced. The combination of graphitic fillers with dimensions on different length scales can potentially form an interconnected multi-dimensional filler network and, thus contribute to enhanced thermal conduction. In this review, we describe the relevant properties of different 2D nano-structured graphitic materials and the factors which determine the translation of the intrinsic thermal conductivity of these 2D materials to epoxy resins. The key challenges and perspectives with regard achieving epoxy composites with significantly enhanced thermal conductivity on addition of 2D graphitic materials are presented.

Contents

1. Introduction

Epoxy-based composites have been developed for a broad range of applications from adhesives, coatings, structural composites to electronic encapsulates due to their good mechanical properties, resistance to environmental degradation, adhesive properties, low shrinkage during curing, good chemical resistance, high electrical insulation, wear resistance and heat resistant properties [1, 2]. However, epoxy resins, like many other polymeric materials are thermal insulators and have low thermal conductivity (λ), typically in the range of 0.15~0.35 W/(mK) [3], which highly limits their applications in thermal management systems. Graphitic fillers, such as zero-dimensional (0D) carbon black, 1D carbon nanotubes (CNTs) and 2D graphene nanoplatelets (GNPs) have intrinsically high λ, significantly higher than all metallic and ceramic fillers, see Table 1. By way of example, the λ for graphene layer(s) has been reported to be between 2000~6000 W/(mK) [3], compared with boron nitride, 185~300 W/(mK) [4-6]. Therefore, the incorporation of 2D graphene or its related carbon derivatives to epoxy resins are expected to improve the λ of composite materials. But in most cases, the measured λ of such composites are significantly below theoretical predictions, because the λ values of such composites is not only dependent on the intrinsic λ of the polymer matrix and filler, but is also determined by the extent of dispersion and distribution of the filler in the polymer matrix, the molecular structure, morphology, surface properties of the filler, as well as the packing density, orientation of the filler and critically the extent of interfacial interactions between filler and polymer matrix.

In this review, the fundamental thermal conductivity of 2D graphitic materials and epoxy resins is described and, the role of 2D graphite and its derivatives, such as expanded graphite (EG), graphene nanoplatelets (GNPs) and graphene oxide (GO) in determining the λ of epoxy based composites is discussed, including, the role of surface properties of the 2D filler and the processing conditions employed during composite preparation on the thermal conduction of the composites. The technical challenges and perspectives in translating the outstanding thermal conductivity of 2D nanostructured graphitic materials to epoxy resins (i.e. polymeric insulators) is addressed.

2. Epoxy resins and 2D graphitic thermally conductive fillers

2.1 Epoxy resins

2.1.1 Classification of epoxy resins

Epoxy resins, also known as poly(epoxides), are a class of reactive oligomers and polymers which contain epoxide groups (Figure 1). Based on the chemical composition, epoxy resins can be grouped in to five types (Table 1):
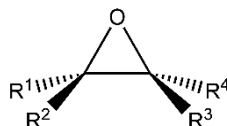
Figure 1. Epoxide group

(1) Bisphenol A (DGEBA); produced from combining epichlorohydrin and bisphenol A to give bisphenol A diglycidyl ethers.

(2) Bisphenol F epoxy resin (DGEBF); bisphenol F may also undergo epoxidation in a similar fashion to bisphenol A. Compared to DGEBA, bisphenol F epoxy resins have lower viscosity and a higher mean epoxy content, which (once cured) gives them increased chemical resistance.

(3) Novolac epoxy resin; reaction of phenols with formaldehyde and subsequent glycidylation with epichlorohydrin produces epoxidized novolacs, such as epoxy phenol novolacs (EPN) and epoxy cresol novolacs (ECN). These are highly viscous to solid resins with mean epoxide functionality of around 2 to 6.

(4) Aliphatic epoxy resin; are typically formed by glycidylation of aliphatic alcohols or polyols. These resins display low viscosity at room temperature (10-200 mPa.s) and are often referred to as reactive diluents.

(5) Glycidylamine epoxy resins; are higher functionality epoxies formed by reacting aromatic amines with epichlorohydrin. These resins are low to medium viscosity at room temperature, which

4

makes them easier to process than EPN or ECN resins. This coupled with high reactivity, plus high temperature resistance and mechanical properties of the resulting cured epoxy network makes them important materials for aerospace composite applications.
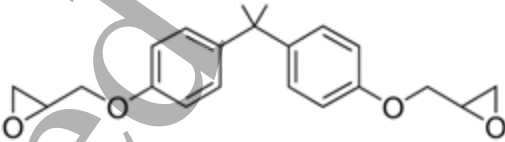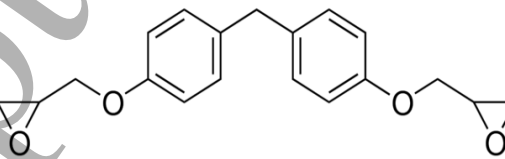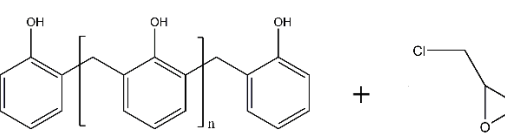
Curing may be achieved by reacting an epoxy with itself (homo-polymerisation) or by forming a copolymer with poly(functional) curatives or hardeners. In principle, any molecule containing a reactive hydrogen may react with the epoxide groups of the epoxy resin. Common classes of hardeners for epoxy resins include amines, acids, acid anhydrides, phenols, alcohols and thiols. Relative reactivity (lowest first) is approximately in the order: phenol < anhydride < aromatic amine < cycloaliphatic amine < aliphatic amine < thiol. The epoxy curing reaction may be accelerated by addition of small quantities of accelerators. Tertiary amines, carboxylic acids and alcohols (especially phenols) are effective accelerators. As with other classes of thermoset polymer materials, blending different grades of epoxy resin, as well as the use of additives, plasticizers or fillers is common to achieve the desired processing and/or final properties, or to reduce cost [7].

Table 1 Thermal conductivity (λ) values for different types of epoxy resins.

Epoxy resins	Monomer	λ (W/mK)
DGEBA		0.15-0.35 [8, 9]
DGEBF		0.2 [10]
Novolac epoxy resin		0.15-0.25 [11-13]

Aliphatic epoxy resin		0.16 [14]
Glycidylamine epoxy resin		N/A
	[15]	
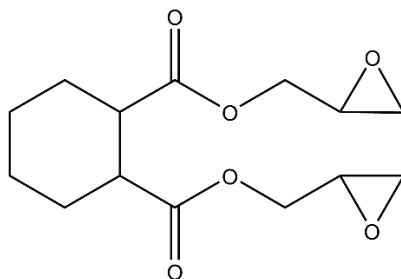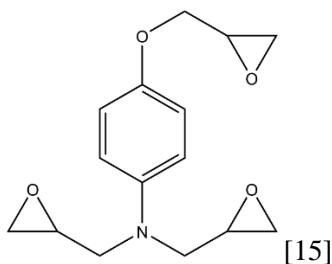
2.1.2 Thermal conductivity (λ) of epoxy resins

Cross-linked epoxy resins are intrinsically brittle and amorphous. Phonons, quantised modes of vibration occurring in a rigid crystal lattice, are the primary mechanism of heat conduction in most epoxy resins since free movement of electrons is not possible [16]. The Debye equation is usually used to calculate λ of polymers, Equation 1:

$$\lambda = \frac{1}{3} C_p . v. l \tag{1}$$

where, C_p is the specific heat capacity per unit volume; v is the average phonon velocity; and l is the phonon mean free path. For amorphous polymers, l is extremely small (i.e. a few angstroms (Å)) due to phonon scattering from numerous defects, resulting in very low λ for polymers [17]. The reported experimental values of λ for epoxy resins varies from 0.06-0.38 W/(mK) [18, 19]. λ for epoxy resins depends on many factors, such as chemical constituents, bond strength, molecular structure, side group molecular weight and type and, strength of defects or structural faults, processing/curing conditions and temperature.

Most commercial epoxy resins such as DGEBA can only form isotropic amorphous morphology, so the relevant λ is very low, between 0.15–0.35 W/(mK). It has been reported that liquid crystalline thermosets can promote the movement of phonons, and thus can lead to resins with higher λ [3]. An

6

epoxy based on diglycidyl ester-terminated liquid crystalline epoxy was reported to have λ up to 0.30-0.39 W/(mK) [20]. In summary, epoxy resins like all polymeric materials are thermal insulators.

2.2 Thermal conductivity (λ) of fillers for polymers

High thermally conductive fillers are introduced into the epoxy matrix in an attempt to enhance λ, including metallic-, carbon- and ceramic-based fillers. The λ of the composites is largely determined by a mechanism of heat transfer between the filler particles. In general, fillers with purely a phonon heat transfer mechanism (as opposed to those having both phonon and electron) have lower λ. Metal oxides, such as Al_2O_3, have a λ around 30 W/(mK) [21]. Even for highly thermally conductive ceramic materials, such as boron nitride and aluminium nitride, λ can reach 100–300 W/(mK) [3, 13, 21]. In contrast, free electrons are much more efficient in transporting heat compared to phonons since electrons are more resistant to scattering and move at higher speeds. Thus, metallic- and carbon-based fillers have much higher λ mainly due to free electrons. Table 2 lists the thermal conductivity of commonly used materials.

Table 2. Thermal conductivity (λ) values of some common materials.

Filler	Category	λ (W/mK)	Reference
Aluminium	Metal	234	[21]
Copper	Metal	386-400	[3, 22]
Silver	Metal	417-427	[3, 23]
Carbon nanotubes	Carbon	1000-4000	[3, 24, 25]
Carbon fibre	Carbon	10-1000	[26, 27]
Graphene	Carbon	2000-6000	[3, 28]
Graphite	Carbon	100-500	[29, 30]
Aluminium nitride	Ceramics	100-319	[3, 31]
Beryllium oxide	Ceramics	230-330	[32]
Boron nitride	Ceramics	185-400	[4, 33]

Carbon-based materials, including carbon nanotubes (CNTs), carbon fibre (CF), graphite and its derivatives (such as graphene) have been widely studied as heat conductive fillers because of their high intrinsic λ (Table 2). Among carbon-based materials, graphene has extremely high λ, which can

7

exceed that of CNTs, as its single layer structure forms effective pathways for heat transfer. It is considered to be an outstanding thermal conductor. Furthermore, compared to other nano-structured carbon materials, sources of graphene like materials are abundant and relatively cheap.

2.3 2D Graphitic materials

2.3.1. Natural graphite (NG)

The crystal lattice of natural graphite consists of stacks of parallel 2D graphene sheets (a single carbon layer in the crystalline honeycomb graphite lattice is known as graphene) with sp^2 hybridised carbon atoms tightly bonded in hexagonal rings. The layered structure of graphite exhibits 3D order, see Figure 2(a). The adjacent graphene sheets in graphite are separated from each other by 0.335 nm, half the crystallographic spacing of hexagonal graphite. The adjacent graphene sheets are held together by van der Waals forces and thus they can easily slide away from each other, which may benefit dispersion and thermal conduction [34].

2.3.2 Expanded graphite (EG)

The layered structure of natural graphite can be intercalated by various atoms, molecules, metal complexes and salts to form graphite intercalation compounds (GICs) [35, 36]. In GICs, the graphene layers either, accept electrons from, or donate electrons to, the intercalated species. Graphite intercalated with electron donors like alkali metals (e.g. potassium and sodium) are known as donor-type GICs, whereas compounds formed by the intercalation of molecular species acting as electron acceptors like halogens, halide ions and acids are known as acceptor type GICs. The acids involved in forming GICs include nitric acid, sulphuric acid, perchloric acid and selenic acid. When GICs are heated past a critical temperature or exposed to microwave radiation, a large expansion (up to hundreds of times) of graphite flakes occur along the c-axis, forming worm-like structures with low density. This 'puffed-up' product is known as exfoliated or expanded graphite (EG) [37-39], as shown in Figure 2 (b).

8

2.3.3 Graphene nanoplatelets (GNPs)

Expanded graphite can be further exfoliated into thinner stacks of sheets by ultrasonication or high speed shearing in solvents. The graphene nanoplatelets (GNPs) obtained are about 30–80 nm thick (or even thinner, see Figure 2 (c)). GNPs possess impressive λ, values up to 3000 W/(mK) have been reported [40]. Apart from exfoliating EG, the most frequently used economical route to preparing bulk quantities of GNPs is via exfoliation of graphite intercalated compounds (GICs). Typically, the process involves the heating of graphite powder with potassium (K) under vacuum to form the GIC. Then, the GIC is reacted with ethanol which reacts with potassium to form potassium ethoxide and hydrogen gas. The evolution of hydrogen gas helps in the partial exfoliation of the graphitic layers to form GNPs. The GNPs produced by this technique generally have 40 ± 15 graphene layers [41] or comprise multiple graphene sheets [42]. In contrast to CNTs, whose production requires intricate and costly manufacturing processes, highly pure GNPs can be derived from available and plentiful sources of natural graphite, using conventional exfoliation methods. Thus, utilisation of GNPs in various engineering applications could be rendered as more cost-effective than higher cost CNTs [43].

2.3.4 Graphene oxide (GO)

Graphene oxide is generally prepared by chemical oxidation and exfoliation of graphite [44], which often follows Hummers' and Offeman methods [45]. The graphite is treated harshly with anhydrous sulphuric acid, sodium nitrate and potassium permanganate in order to generate oxygen-containing functional groups on the carbon surface. As shown in Figure 2 (d), the GO generally contains epoxide and hydroxyl groups on the basal plane surface of the carbon sheets and, carboxyl and carbonyl groups at the edges. The presence of hydroxyl, carboxyl and epoxide groups improve the dispersibility of GO in polar solvents and water [46]. Chemical reduction of GO is carried out by using reducing agents like hydrazine or hydrazine derivatives to convert the electrically insulating GO layers back to conducting graphene. Thermal reduction of GO, involves rapidly heating GO in an inert (argon or nitrogen) environment to produce thermally reduced expanded graphene oxide (TRGO), which is a black powder of very low bulk density [47]. Due to their wrinkled nature, TRGO do not

9

collapse back to GO but remain highly agglomerated (Fig.2 (e)). TRGO can be dispersed by ultrasonication in appropriate solvents, such as N-methylpyrrolidone, dimethylformamide, 1,2dichlorobenzene, nitromethane or tetrahydrofuran. The presence of oxygen groups on the surface of TGRO promotes interaction with polar polymers. SEM of dry, as-produced TGRO powder is shown in Figure 2 (e) [48]. It is worth highlighting that high temperature treatment of free standing GO films up to 1000ºC can significantly increase the in-plane λ at RT of these films, up to ~60 W(mK). Work by Renteria et al. described the production of GO films with very strong anisotropy of λ (λ/λ⊥ ≈ 675), higher than that observed for graphite. Theoretical studies by the same group predicted that λ as high as 500 W (mK) is possible with increased sp^2 domain size and reduced oxygen content [49]. The preparation methods, average sheet dimensions and λ of the different 2D graphite fillers are compared and shown in Table *3*.
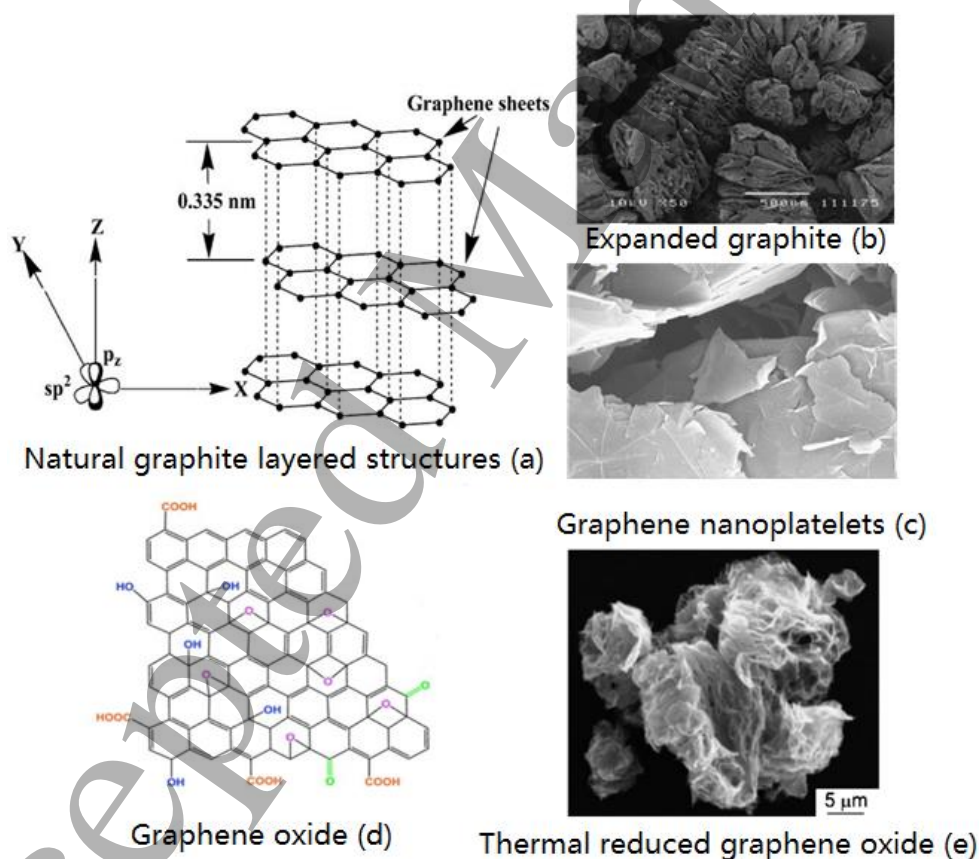

Figure 2. a) Structure of 2D natural graphite [34], b) SEM image of expanded graphite (EG) [50], c) SEM image of graphene nanoplatelets (GNPs), d) representative chemical structure of graphene oxide (GO) [51] and e) SEM image of thermally reduced GO (TRGO) [48].

Table 3. Preparation methods, geometry and λ values of 2D graphitic materials

Filler Type	Preparation methods	Lateral Dimension	Thickness	λ W/(mK) (In-plane)
Natural graphite (NG)	Crushing and grinding of ore to release entrapped flake, and mined	3-500 μm (Asbury Carbons)	100 μm (270-520 μm) [29]	100-500 [29, 30]
EG	Pretreating natural graphite with chromic acid or concentrated sulphuric acid, expanding the graphite assisted by thermal shock or microwave.	μm	100-400 nm	N/A
GNPs	Further exfoliating EG into thinner stacks of GNS by ultrasonication or high speed mixing in solvents. Or heating graphite powder with K under vacuum to form the graphite intercalated compounds (GIC). GIC reacted with ethanol which reacts with K to form K ethoxide and hydrogen gas. The evolution of hydrogen gas helps in the partial exfoliation of the graphitic layers to form GNPs.	μm	30–80 nm or even thinner	Up to 2800 [52]
GO	Natural graphite is treated harshly with anhydrous sulphuric acid, sodium nitrate and potassium permanganate in order to generate oxygen-containing functional groups on the carbon surface.	μm	>1 nm	Up to 872 [53]

3. Measurement of thermal conductivity

3.1 Mechanism of thermal conduction in epoxy resins

Heat transfer in polymers is governed by thermal conduction. At the microscopic scale, heat conduction rapidly moves or vibrates the crystal lattice by interacting with neighbouring vibrating lattices, transferring some of their energy (heat) to neighbouring particles. For amorphous or semi-crystalline polymers, including epoxies, heat conduction is very low because phonon scattering mainly occurs in the amorphous phase [3].

3.2 Methods used for measurement of thermal conductivity of epoxy composites

(1) Steady state measurement

Steady state conduction is a form of conduction that occurs when the temperature difference driving conduction is constant, so that after an equilibration time, the spatial distribution of temperature in the conducting object does not change any further. In steady state conduction, the amount of heat entering a section is equal to the amount of heat coming out. The law of heat conduction, also known as Fourier's law, states that the time rate of heat transfer through a material is proportional to the negative gradient in the temperature and to the area, at right angles to that gradient, through which the heat flows. The differential form of Fourier's law of thermal conduction shows that the local heat flux density, q, is equal to the product of λ, and the negative local temperature gradient, −∇T. The heat flux density is the amount of energy that flows through unit area per unit time:

$$q = -\lambda . \nabla T \qquad (2)$$

where (including the SI unit), q is the local heat flux density, W/m^2, λ is the material conductivity, $W/(mK)$ and, ∇T is the temperature gradient, K/m. λ is often treated as a constant, though this is not always true. While λ of a material generally varies with temperature, the variation can be small over a significant temperature range for common materials. In anisotropic materials, λ typically varies with orientation and, in this case λ is represented by a second-order tensor [16]. For example, a bar may be cold at one end and hot at the other, but after a state of steady state conduction is reached, the spatial gradient of temperatures along the bar does not change any further, as time proceeds. Instead, the temperature at any given section of the rod remains constant, and this temperature varies linearly in space, along the direction of heat transfer. In steady state conduction, all the laws of direct current electrical conduction can be applied to "heat currents".

Classical steady state methods, such as "guarded hot plate", measure the temperature difference across the specimens in response to an applied heating power, either as an absolute value or by comparison with a reference material put in series or in parallel to the sample to be measured [10, 54]. Normally, a sample of unknown conductivity is placed between two samples of known conductivity (usually brass plates). The setup is typically vertical with the hot brass plate at the top, the sample in between the cold brass plate at the bottom. Heat is supplied at the top and made to move downwards

to stop any convection within the sample. Measurements are taken after the sample has reached the steady state (with zero heat gradient or constant heat over entire sample). However, these methods are often time consuming and require relatively bulky specimens.

(2) Non-steady state measurement

In general, during any period in which temperature changes with time at any place within an object, the mode of thermal energy flow is termed transient conduction. Another term is "non-steady state" conduction, referring to time-dependence of temperature fields in an object. Non-steady-state methods to measure λ do not require the signal obtained to be a constant value. Instead, the signal is studied as a function of time. The advantage of these methods is that they can in general be performed more quickly, since there is no need to wait for a steady-state situation. The disadvantage is that the mathematical analysis of the data is more difficult. If the conducting body has a simple shape, then exact analytical mathematical expressions and solutions may be possible [16]. However, most often, because of complicated shapes with varying λ within the shape of interest, numerical analysis is required using a computer. Non-steady state methods for measurement of λ include transient plane source, hot wire and laser flash techniques [55-57]. Among these, laser flash thermal diffusivity measurement is widely used, being a relatively fast method using small specimens [14, 58-59]. In this method, the sample surface is irradiated with a very short laser pulse and the temperature rise is measured on the opposite side of the specimen, permitting calculation of the thermal diffusivity of the material. λ is then calculated using Equation (3):

$$\lambda = \alpha \cdot C_p \cdot \rho \tag{3}$$

where α, C_p and ρ are the thermal diffusivity, heat capacity and density, respectively. Significant experimental error may be involved in λ measurements, due to difficulties in controlling test conditions, such as the thermal contact resistance with the sample, leading to accuracy in the measurement of λ of typically in the range $\pm$ 5$-$10%. In indirect methods, such as those calculating λ from thermal diffusivity, experimental errors with respect to density and heat capacity values will also contribute to experimental error in the value of λ determined [3].

13

In summary, steady state methods are time consuming and require relatively bulky specimens, while transient methods are relatively fast using small specimens. A wide range of thermal conductivity, from 0.01-1800 W/(mK), can be measured by non-steady methods which are also suitable for most polymers and polymer composites [60-61]. Among these, laser flash thermal diffusivity measurement is most frequently used.

3. Preparation and thermal conductivity measurement of epoxy composites containing 2D graphitic fillers

The manufacture of composites of epoxy and 2D fillers involves choosing an appropriate blending method to attain satisfactory dispersion and distribution of the filler throughout the epoxy matrix. Various dispersion techniques that have been employed to manufacture composites of epoxy and 2D graphitic materials are summarised as follows.

4.1 Methods employed to prepare composite of epoxies and 2D graphitic materials

4.1.1 In-situ polymerization

The monomer (and/or oligomer) is polymerized in the presence of the 2D filler and consequently the *in-situ* technique facilitates stronger interactions between the 2D filler and the polymer phase. However, this method may not be effective for the mass production of such composites. Zhou *et al*. reported that λ of a composite of an epoxy and multilayer GO with 2 wt% GO (8.4 nm thick, 17 layers) loading reached only 0.63 W/(mK) [62].

4.1.2 Solution blending

In solution blending, the polymer is dissolved in a solvent and the 2D filler is dispersed in the resulting solution by sonication and/or mechanical stirring. The solvent is then removed and the bulk polymer material containing the 2D filler is usually moulded to give the shape required. This technique is the most frequently used and it also results in homogeneous dispersion of the 2D filler in the epoxy. The disadvantage of this method is the use of large amounts of organic solvent and the associated environmental concerns due to the removal of the solvent which have prevented the

14

adoption of this technique for the large scale fabrication of epoxy based composites. Table 4 lists the

λ of composites of epoxy and graphitic materials prepared by this method. Supercritical carbon

dioxide (scCO$_2$) has been employed to aid incorporation of GNPs and multi-walled carbon nanotubes

(MWCNTs) into an epoxy matrix, to enhance both electrical and thermal properties of the epoxy [63].

The percolation threshold for electrical conductivity for the composite was 2wt%, one-third that

obtained when acetone was used. However, the authors did not compare λ of the composites prepared

by both methods. The proposed scCO$_2$ mixing process not only aids dispersion of GNPs and

MWCNTs in the epoxy but also eliminates the presence of solvent after decreasing the pressure. In

work report by Veca *et al.* [64], expanded graphite (EG) could be further exfoliated in a solution

blending process (sonication and mechanical stirring) to produce nm size carbon structures ("carbon

nanosheets"). These carbon nanosheet(CNS) materials were used as fillers for polymers that

exhibited relatively high λ, 80 W/(mK) for a volume fraction of 0.33.

Table 4. Thermal conductivity (λ) of composites of epoxy and 2D graphitic materials prepared by solution blending

Filler composition (mixing technique)	λ (W/mK)	Epoxy type	Filler size and surface treatment	Reference
1.525wt% MWCNTs + 4.575wt% GNPs (ScCO$_2$ assisted magnetic stirring)	0.23-0.89 (laser flash LFA447)	DGEBA (5000-6000 cps)	Size:550nm, thickness: 8 nm, specific surface area:100 m^2/g Supercritical CO$_2$-assisted mixing to prepare graphene/CNTs/epoxy composites	[63]
33vol% CNS (sonication + stirring)	80 (thermal diffusivity by laser heating angstrom method)	EPONOL resin 53-BH-35, DGEBA	6-7nm thick. The supplied exfoliated graphite was retreated with alcohol and oxidative acid, then vigorously sonicated into thinner nanosheets	[64]
1wt% graphene nanosheets 1wt% GO coated PMMA nanoballs (sonication with acetone	0.2-0.66 0.2-1.4(steady state 1-D heat conduction	Epon 862 (DGEBF)	The nanoballs were coated with chemically reduced GO to form a core-shell additive and dispersed in epoxy	[54]

+shear mixing)	method)			
(1) 30wt% 3D graphene (2) 30wt% reduced GO (3) 30wt% natural graphite (ultrasonic + stirring)	(1)0.25-4.9 (2)0.25-4.2 (3)0.25-1.6 (laser flash method)	N/A	3D graphene was prepared by CVD	[65]
3wt% chemical reduced GO (ultrasonic + mixing)	1.192 (hot disk method)	DGEBA	Thickness:5-50nm with crumpled silk waves of graphene sheet, Al and KOH to reduce graphene oxide	[6]
4phr graphene nanosheet (sonication + stirring)	0.2-1.91 (hot disk method)	DGEBA (NPEL-128)	Lateral dimension: $9\times7\mu m$ Thickness:2.3-5.1nm Non-covalent functionalized-poly(glycidyl methacrylate) containing localized pyrene groups(Py-PGMA)	[67]
12wt% graphene flakes (sonication + mixing)	0.2-0.73 Thermal impedance (Quickline 10-C)	Stycast1266	Size: 1.5-10 μm, Thickness: 12nm (30-50 layers), Specific surface area:80 m^2/g.	[68]
2vol% synthetic diamond 2 vol% GNPs (ultrasonic agitation)	0.15-0.380.15-0.33(hot disk method)	Epon8281, Hexion	GNPs flaky with size: 50μm thickness<10nm. Synthetic diamond with size<10μm, 2vol% GNPs created more agglomeration than diamond.	[69]
1vol% GNPs (stirring /solution blend)	0.17-0.24 Perpendicular 0.17-0.6 Parallel (laser flash)	N/A	Thickness: 8nm (3-5 layers) Fe_3O_4 coated GNPs, magnetic alignment.	[70]
3wt%MWCNTs 3wt% GNPs 15wt% GNPs	0.29-0.36 0.29-0.41 0.29-0.8	Low viscosity Araldite LY1556,	GNP size:5μm thickness:10-12nm (20-25 layers)	[71]

16

(mixing)	TCI Mathis	Hardener Aradur1571		
3wt%MWCNTs	0.21-0.33	DGEBA	GNPs size: 15 μm	[72]
3wt%GNPs	0.21-0.47		Thickness:11-15 nm	
	Hot disk			

4.1.3 Milling

Traditional mixing equipment such as ball milling and 3-roll milling can be adopted for blending operations (

Table *5*). Guo *et al*. [73] prepared composites of epoxy and GNPs by two methods: ball milling and sonication. Different mass fractions (between 5–25 wt%) of GNPs were dispersed in acetone solution containing 15 wt% epoxy resin with the help of sonication for 0.5 h at room temperature (RT). The suspension was placed in a stirring basket-ball milling machine and mixed at a speed of 300 rpm at RT for a period between 6 h and 36 h. Similarly, the different mass fractions (i.e. 5–25 wt% loading) of GNPs were dispersed in acetone solution containing 15 wt% epoxy with the assistance of sonication. From the SEM images in Figure 3 (a) the GNPs can be seen to be interconnecting and dispersed uniformly throughout the epoxy matrix. In contrast, many graphite sheets are in the form of agglomerates in Figure 3 (b). The structure of composites prepared by ball milling as shown in Figure 3 (a) was more uniform such that the phonon scattering processes especially for the GNPs added to the epoxy matrix were minimised.

Table 5. Thermal conductivity (λ) of composites of epoxy and 2D graphitic materials prepared by ball milling

Filler (mixing technique)	λ (W/(mK))	Epoxy	Filler size and surface treatment	Reference
1wt%MWCNTs +	0.24-0.34	CYD-128	Size: hundreds of nanometres to tens of micrometres	[74]
1wt%GNPs (3-roll mill, gap	(DRL-III		Thickness:2-4 nm(8 layers)	

5μm, 270 rpm)	TC meter)			
1wt% TRGO (3-roll mill)	0.154-0.2025 (hot disk method)	DGEBA (Epon828)	More oxygen-containing groups in TRGO, better dispersion, higher λ	[75]
5wt% GNPs (3- roll mill, 200rpm)	0.12-0.7 (Laser flash)	MVR444	Aspect ratios up to 300–1000 and thicknesses of 5–17 nm	[76]
(1)25 wt% GNPs- (ball milling) (2)25 wt% GNPs- (sonication)	(1)0.2-2.67 (2)0.2-1.4 (C-therm TiC)	N/A	Thickness:30-80nm (<10 layers)	[73]
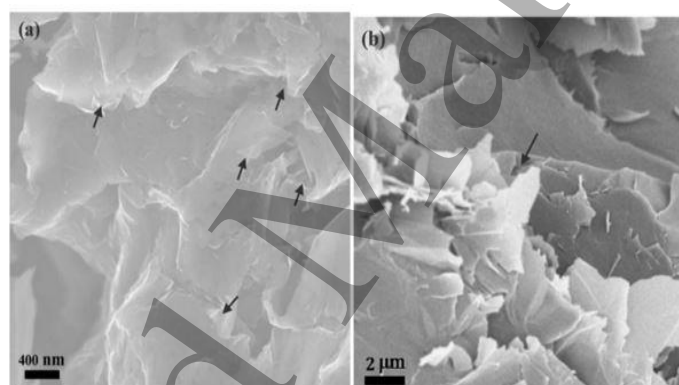
Figure 3. SEM images of the fractured surface of composites of epoxy and GNP prepared by (a) ball milling induced exfoliation and (b) sonication. Both samples contain 25 wt% GNP and were milled or sonicated for 24h. (Arrows indicate the location of the platelets) [73].

As shown in Figure 4 (a) the GNPs tend to form stacks of graphitic structures. The cross-section of the same specimens showed the layered structure of the GNPs in Figure 4 b). Individual layers could be seen in Figure 4 (c). Individual single atomic carbon layers (corresponding to monolayer graphene sheets) dominated by one dark line with a thickness of 0.5 nm were identified, suggesting that composites contained a number of single and few-layer graphene sheets, see Figure 4 c) and (d).

18
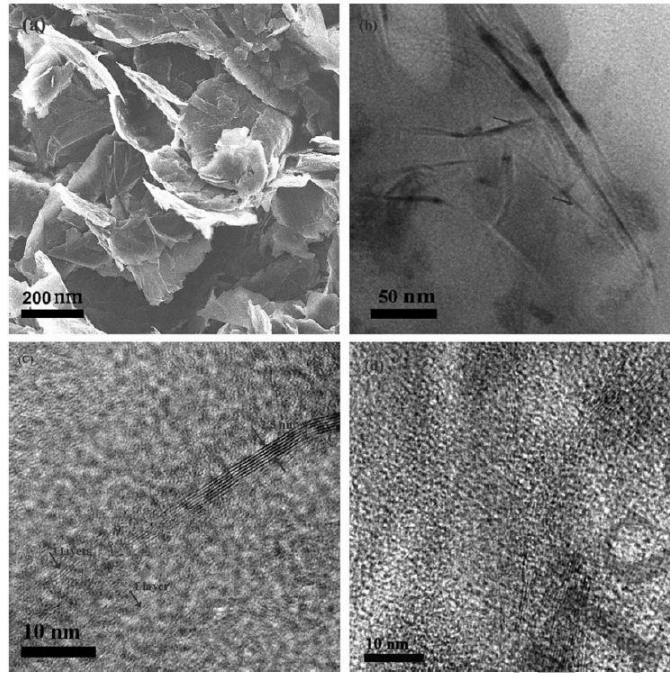
Figure 4. (a) SEM image of graphene in solid state and (b, c and d) HRTEM images of GNPs embedded in epoxy resin. These samples (25 wt% loading) were prepared subjected to treatment times of 24 h (a, b, c) and 6 h (d), respectively [73].

The λ of the composite prepared by ball milling increased from 0.2 to 2.67 W/(mK) on addition of 25 wt% GNPs, while the λ of the composite prepared by sonication method increased from 0.2 to 1.4 W/(mK). Two reasons were proposed to explain this enhancement: (i) the better homogeneous dispersion of GNPs in the polymer could possess better thermal conductance and (ii) the high quality and better exfoliation of GNPs (from TEM) could promote better thermal conductance, resulting in increased contact surface area between GNPs and the polymer matrix improving phonon transport in the composite.

4.1.4. Combination of different mixing techniques

Table 6 lists the λ values of various polymer/graphite composites prepared by a combination of solution compounding with one or more of the following procedures: sonication, shear mixing or calendaring. This combinatorial approach involving various techniques becomes necessary when the system viscosity increases rapidly as solvent content decreases as in the case when working with epoxy matrices. This is a promising approach, as it can mitigate the problems faced in each of the individual mixing techniques, while harnessing the advantages of each.

19

Table 6. Thermal conductivity (λ) of composites prepared by combing mixing techniques

Filler	λ (W/mK)	Epoxy type	Mixing techniques	Reference
5wt% GNPs	0.21-0.47	Epon828	Ultra-sonication + shear mixing + 3-roll calendaring	[77]
10wt% GNPs	0.15-0.65	DGEBA(LY556) XB3473	Sonication +calendaring	[8]
8wt% GNPs	+210%	DGEBA Araldite LY556 and XB3473 (Amine hardener)	Ultra-sonication + 3-roll miller (250rpm, gap:5μm)	[78]
(1) 2wt% GNPs (D^a:25μm)	(1) 0.375-0.7	EPIKOTE 828LVEL	Mechanical mixing with solvent + 3-rollmill calendaring	[79]
(2) 2wt% GNPs (D:5μm)	(2) 0.375-0.5	EPIKURE3402		
(1) 3wt% GNPs (D:5μm)	(1) 0.2-0.49	DGEBA-Epon828	Sonication +calendaring	[80]
(2) 3wt% GNPs (D<1μm)	(2) 0.2-0.29	(90wt%epoxy+ 10wt%CTBN)		
0.5wt%TEPA-GO	0.35-0.71	DER331(DOW)	Mixing + 3-roll mill	[9]
0.5wt%raw-GO	0.35-0.59	liquid DGEBA Triethylenetetramine hardener		
2wt% GNPs	0.221-0.415	Araldite LY564(DGEBA) Aradure2954 hardener	Mechanical stirrer + 3-roll mill calendaring	[81]

^{a}Dimension (average diameter).

Ahmadi *et al*. used a combination of techniques (mechanical stirring and 3-roll mill calendaring) to prepare composites of an epoxy and GNPs [81]. The GNPs were first dispersed into the epoxy resin and hardener using a mechanical stirrer. The mixed GNP-resin slurry was then further processed by passing through a 3-roll mill. The dispersion of the GNPs was promoted with three different roller gap

20

distances of 20, 40, and 60 μm. The value of λ increased from 0.221 (neat epoxy) to 0.355 W/(mK) for a gap distance of 20 μm with 2wt% GNPs. A higher λ was obtained (0.415 W/mK) when a gap distance of 40 μm was used, this can be ascribed to the higher aspect ratio of the GNPs used. Since the larger sized GNPs could most likely create a more effective conductive network as a result, the λ of the composites with the larger diameter GNPs is higher than those reinforced with relatively smaller GNPs.

5. Relationship between 2D filler structure and thermal conductivity

The λ of epoxy composites containing 2D graphitic fillers are affected by many factors, such as filler type, morphology, orientation, size, aspect ratio and interfacial thermal contact resistance (ITR). The effect of each factor on λ will be discussed in this section.

5.1 Effect of different types of 2D graphitic fillers

Esposito Corcione *et al.* prepared several composites by dispersing three different types of 2D graphitic materials: expanded graphite (EG), commercial GNPs and natural graphite (NG), in a commercial epoxy [82]. 3 wt% EG, GNPs and NG were added to the same epoxy resin using sonication and mechanical mixing techniques. The λ was increased from 0.274 (neat epoxy) to 0.9, 0.46 and 0.31 W/(mK) on addition of EG, GNP and NG, respectively. The greatest increase was obtained for epoxy/EG composites, suggesting a better dispersion and distribution of the filler in the matrix and strong polar interactions between the filler and the matrix, which are attributed to the partially oxidized surfaces of the EG used. Fu *et al*. also reported an enhancement in λ of epoxy composites filled with graphene sheets, graphite flakes and NG [83]. These results show that additions of graphene sheets gave the greatest increment in λ for the composites, which are summarized in Table 7.

21

Table 7. Thermal conductivity (λ) of composites of epoxy and 2D fillers having of varying size.

Filler (mixing techniques)	λ (W/(mK)) (measurement method)	Epoxy type	Filler size	Reference
(1) 3wt% EG	(1) 0.274-0.9	Epikote828	NG, D[a]: 10μm	[82]
(2) 3wt% GNPs	(2) 0.274-0.46	Isophorondiamine	Cluster size: 60μm	
(3)3wt% NG	(3) 0.274-0.31		EG, D:10μm	
(Sonication+mechanical mixing)	(Transient plane technique)		GNPs, D:70μm, T[b]:10-12nm, 20-25 layers, SSA[c]:100m²/g	
(1) 10.1wt% GNS	(1) 0.17-4.01	N/A	(1) D:10μm, T: 1.5nm	[83]
(2) 16.81wt% graphite nano-flake	(2) 0.17-1.84		(2) T: 20nm (50 layers)	
(3) 44.3wt% NG	(3) 0.17-1.68		(3)D:70μm	
(mechanical mixing)	(Hot disk)			

[a]Dimension (average diameter), [b] Thickness and [c] Specific surface area.

5.2 Effect of filler geometry and morphology

5.2.1 Lateral dimensions

Two types of GNPs with different lateral dimensions (GNP-C750 with diameter <1μm, thickness of 5-7nm, and GNP-5 with diameter of 5μm, thickness of 5-7nm), were separately incorporated into an epoxy resin [80]. 10wt% carboxyl terminated butadiene acrylonitrile (CTBN) was added to the epoxy to improve the fracture toughness. The study showed that GNP-5 was more favourable for enhancing the properties of the epoxy/CTBN matrix. As the GNP concentration was increased to 3wt%, GNP-5 resulted in a greater improvement in λ of 145% compared to the neat matrix, from 0.2 to 0.49 W/(mK). While for the GNP-C750 filled composites, the improvement in λ was only 47%, from 0.2 to 0.29 W/(mK). The difference is ascribed to the larger aspect ratio and improved dispersion of GNP-5 in the matrix. Compared with GNP-C750, the GNP-5 flakes can be dispersed and distributed in the matrix with fewer agglomerations creating a more effective conductive pathway for phonon conduction. Furthermore, for a given amount of GNP-5 and GNP-C750, the authors proposed that there is less effective interfacial interaction between GNP-5 and the

22

matrix, due to the larger aspect ratio of GNP-5. As a result, less phonon scattering occurred at the GNP-5 matrix boundaries, resulting in a greater enhancement in λ compared to the GNP-C750 composites. Chatterjee *et al.* also prepared composites with epoxy and two types of GNPs having different lateral sizes (i.e., 25 μm and 5 μm), and they came to a similar conclusion [79]. The enhancement in λ of the composite with 25 μm GNP was greater (from 0.37 to 0.7 W/(mK)) than that of the composite with the 5 μm GNP (from 0.37 to 0.5 W/(mK) at 2wt% loading). Five types of GNPs with lateral size in the range of 2 to 34 μm were incorporated into an epoxy resin and, λ increased with increasing lateral size from 2 to 20 μm. The composite with a high λ of 12.4 W/m K (vs 0.2 W/m K for neat resin) was achieved by incorporating 24 vol% 20 μm GNPs into the epoxy resin [84, 85]. The defects in the GNP sheets also contributed to phonon scattering, which resulted in the lower λ for the composite with 34 μm GNP as compared to the composite with the 20 μm GNP.

5.2.2 Filler thickness

Un-modified graphene oxide nanoplatelets (GONPs) with comparable dimensions but different thicknesses, i.e. rigid-GONP (thickness: 34 nm, diameter: 17 μm) and flexible-GONP (thickness: 7 nm, diameter: 19 μm), were used to reinforce an epoxy resin [86]. Both rigid- and flexible-GONPs were equally well-dispersed in the epoxy matrix. Addition of r-GONPs to the epoxy resulted in a higher λ (from 0.2 to 0.75 W/(mK)) for a loading of 3 wt% r-GONPs) than that on addition of f-GONPs (from 0.2 to 0.35 W/(mK) with 3 wt% f-GONPs loading). The superiority of r-GONP in promoting heat conduction was associated with there being "more" inside-layers that act as heat-conductive channels, while "fewer" outside-layers (due to lower number of r-GONPs for an equivalent weight fraction) transfer phonons from r-GONPs to the epoxy matrix via interfacial hydrogen bonding. The authors proposed that bonded interfaces cause the damping of phonons when the matrix is a poor conductor, and thus degrade the efficiency of the conductor in insulator-conductor systems. However, in work by Kim *et al.*, EG was prepared by a rapid expansion method (inductively coupled plasma). The volume expansion can be controlled by the treatment temperature and time and as such thinner EGs can be obtained via higher volume expansion. These worker's found that λ of the composites increased with increasing expanded volume of the filler, for the same filler content. Based

23

on a quantitative analysis of filler size within the composites using non-destructive micro-computed tomography, the larger size of a three dimensional (3D) thermally conductive filler network with respect to the volume expansion were confirmed. Composites containing 20 wt% EG treated at 800 °C showed the highest λ at 10.77 W/mK, an improvement of 5883% compared to the value of 0.18 W/mK cited for pure epoxy resin when the thermally conductive EG filler network was generated in 3D [87].

5.2.3 Filler aspect ratio

A further factor dramatically affecting λ is filler aspect ratio (i.e. the ratio of average diameter to thickness) of 2D graphitic materials. Shahil *et al.* demonstrated a significant increase in λ of composites of GNPs and an epoxy for a GNP volume fraction of 0.1 (from 0.2 to 5.1 W/(mK)) [88]. The GNPs used were monolayer or bilayer (~90%) with lateral dimensions in the range 50 nm to 0.5 μm. The high aspect ratio is in part responsible for the significant increase in λ. The importance of aspect ratio can be understood physically in that increasing the length of the lateral dimension of the GNPs shifted the phonon dispersion towards lower frequencies. Since the large acoustic mismatch between the GNP–epoxy interface causes inelastic phonon scattering, using large aspect ratio GNPs improved the thermal transport across the GNP–epoxy interface by reducing phonon scattering at the interface. Chu *et al.*, Sha *et al.* and Ahmadi *et al.* all reported similar conclusions for their studies [81, 89-90].

5.2.4 Filler morphology

In the work described in section **5.2.2** [86], other factors also further weaken the reinforcing capability of f-GONP such as: (i) wrinkle/scroll structures of the flexible 2D graphitic morphology reduced both dimensionality and the effective aspect ratio of f-GONP; (ii) small wrinkles scatter phonons with short wavelength, while large scrolls scatter long wavelength phonons, and (iii) such 'waviness' adds interfacial thermal resistance (i.e. ITR, phonon acoustic mismatch increased with decreasing filler radius). The waviness effect (surface morphology) of GNPs on λ of GNP-based composites was also investigated by Chu *et al*. [89]. Two types of GNPS, 'wrinkled' GNPs (w-GNPs)

24

and 'flat' GNPs (f-GNPs) were used to fabricate GNP/epoxy composites. Applying the same processing conditions, f-GNPs exhibited a higher enhancement in λ (from 0.19 to 1.16 W/(mK)) than that for w-GNPs (from 0.19 to 0.9 W/(mK)) for a 10 vol% loading. This might be because the waviness of the GNPs can be considered as structural defects formed during oxidation and at high temperatures. Such wrinkling-related defects are the source of phonon scattering, leading to the low thermal enhancement of w-GNPs in these composites [89, 91].

5.3 Effect of surface functionalization of 2D graphitic fillers

To avoid filler agglomeration during mixing with epoxies and to enhance interfacial bonding between the 2D filler and polymer matrix, functionalisation is usually helpful to disperse graphene and its' derivatives in polymers. Functionalisation of 2D graphitic fillers may significantly affect λ of polymer/filler composites by changing the λ of the filler, the thermal contact between adjacent filler sheets/platelets in a network and the interfacial thermal resistance between filler and polymer, as well as aiding filler dispersion and distribution throughout the polymer matrix. Functionalisation can be achieved by covalent and non-covalent methods with different chemical approaches (Table 8) [92], such as with different chemical groups, surfactants, polymers and metals. Amine-terminated poly(butadiene-co-acrylonitrile) [93], methanesulfonic acid / ɤ-glycidoxypropyltrimethoxysilane (MSA/KH-560) [94-95], vinylcarbazole - glycidyl methacrylate (containing epoxy group) [96], and aminopropylisobutyl polyhedral oligomeric silsesquioxane were used to functionalize GNPs [97]. The surface functionalized GNPs can further improve the λ of the composites, which is associated with reduced filler (GNP) agglomeration. With increasing addition of GNPs, the corresponding thermally conductive channels of GNPs to GNPs are more easily formed. For a given GNP loading, functionalized GNPs possess better interfacial compatibility and lower interfacial thermal resistance with the epoxy resin, favourable for phonon transport and further increasing the λ of the composite material.

Metals have also been used to functionalize GNPs, including Ag nanoparticles (30-50 nm thick) to decorate graphene nanosheets. On addition of 5 wt% of these Ag nanoparticles to an epoxy, a λ of 1

W/(mK) was obtained [98]. Bimetallic Co-Fe nanoparticle coated GNPs increased the λ of an epoxy to 4.7 W/(mK) in-plane and to 2.5 W/(mK) through plane, with addition of 17 wt% GNPs and 3 wt% CNTs, respectively [99].

Amines, Al_2O_3, $Al(OH)_3$, gallic acid, saline, epoxide and carboxylic acid, have also been used to functionalize GNPs [19, 100-104]. The attachment of polar groups such as $COOH^-$, NH_2^-, or OH^- to GNPs promotes interactions with epoxy resins, and permits fabrication of a composite containing a high concentration of this hybrid filler. For example, a bio-based epoxy monomer (GA-II) was synthesized from a renewable gallic acid. The aromatic group made it capable of being adsorbed on to the surface of graphene via strong π–π interactions. The GA-II anchored graphene was easily and homogeneously dispersed in the epoxy resin and, λ was improved 12 fold for a 2wt% loading, from 0.15 to 1.8 W/(mK) [102].

Chiang *et al.* investigated the influence of non-ionic surfactants on the properties of cured GNP/epoxy composites [105]. The strong π–π interaction between graphene sheets made it very difficult to disperse them homogeneously in some organic solvents and polymer matrices, creating a challenge to form a continuous conductive network in the polymer matrix. As graphene is hydrophobic, it readily aggregates in solvents and in polymer matrices. To overcome this problem, non-ionic Triton X surfactants was added to the GNP/epoxy composite. The structure of Triton X surfactants consists of both a hydrophilic polyethylene oxide (PEO) group and hydrophobic hydrocarbon groups, e.g. *p*-(1,1,3,3-tetramethylbutyl)-phenyl. GNP/epoxy composite containing 13 wt% filler had the highest λ (1.7 W/mK).

Table 8. Thermal conductivity (λ) of composites of functionalized GNPs and epoxy

Filler/(mixing technique)	λ W/(mK)	Epoxy type	Filler size and surface treatment	Reference
5wt% GNPs (high-speed shear mixer, 3000rpm)	0.21-0.5 (Laser flash)	DGEBA (Epon828)	D^a: 5μm, T^b:<10nm, SSA^c:150 m^2/g Amine-terminated poly(butadiene-co-acrylonitrile) modified GNPs	[93]

26

30wt% GNPs (mixing)	0.2-1.698 (Hot disk)	E-51	D:40μm, aspect ratio: 250, GNP surface functionalized with methanesulfonic acid / ɤ-glycidoxypropyl trimethoxysilane (MSA/KH-560)	[94]
30wt% GNPs (mixing/casting)	0.234-1.487 (Hot disk)	Phenylphos phonate-based flame-retardant epoxy resin	D:40μm, aspect ratio: 250, GNP surface functionalized with methanesulfonic acid / ɤ-glycidoxypropyl trimethoxysilane (MSA/KH-560)	[95]
1wt% GNS (ultra-sonication)	0.19-0.45 (Hot disk)	DGEBA (E-51) MeHHPA	vinylcarbazole-glycidyl methacrylate (containing epoxy group) functionalized graphene nanosheets	[96]
0.5wt% graphene (ultra-sonication + mixing)	0.221-0.349 (Laser flash)	N/A	Aminopropylisobutyl polyhedral oligomeric silsesquioxane coated graphene	[97]
10wt% graphene (sonication)	0.2-1.53 (Laser flash)	DGEBA (Epon862), SEIKA-S	D:200nm, T<5nm Non-oxidized graphene flakes with non-covalent functionalisation	[104]
13wt% graphene powder (triple-roller mill-6 millings)	0.2-1.7 (Hot disk)	UVR-6110	D:17μm, T<50nm, SSA:20 cm^2/g Triton X surfactants with polyethylene oxide groups	[105]
5wt% Ag coated graphene nanosheet (ultrasonic + mixing)	0.255-1 (transient plane source principle)	N/A	Ag(30-50nm thick) decorated graphene nanosheets	[98]
17wt% GNPs + 3% wt% CNTs (shear mixer)	Up to 4.7 in plane Up to 2.5 through plane (Laser flash)	DGEBA (KFR-120) KFH-150	D:25μm, SSA:120-150m^2/g Fe-Co coated GNPs by electro-less plating, via bimetallic nanoparticle decoration on the GNP surface and subsequent CVD.	[99]

27

5.6vol% GNPs	0.21-1.62 Light flash	NPEL-128 DDM	Al$_2$O$_3$ coated GNPs using nucleation and hydrolysis of Al(NO$_3$)$_3$ precursor followed by calcination.	[100]
3wt% Al(OH)$_3$ coated GONS (ultrasonic +mixing)	0.188-0.358 (Laser flash)	DGEBA (Kukdo) DDM	Al(OH)$_3$ coated GO by sol-gel method.	[101]
2wt% GNPs (mechanical mixing)	0.38-0.51 (Laser flash)	EPIKOTE 828LVEL	Amine functionalized expanded GNPs	[19]
10wt% GNPs (Sonication)	0.158-3.138 Guarded heat flow meter method	DGEBA (triethylenet etramine	Epoxide functionalized GNPs	[106]
2wt% GA-II/graphene (sonication-100W)	0.15-1.8 (Laser flash)	DER331 (DOW) liquid DGEBA	D: several micrometres, T: 2nm with wrinkled surface. SSA: 700m^2/g (3-4 layers). Gallic acid based epoxy monomer was used and absorbed onto graphene surface.	[102]
68wt%Al$_2$O$_3$ + 7wt% GNPs + 5wt% Mg(OH)$_2$ (solution mixing/cast/cure)	0.2-2.2 (ECO HC-110 thermal meter)	DGEBA MHHPA	Silane grafted GNPs, synergistic effect for flame retardancy	[103]

^{a}Dimension (average diameter), ^{b}Thickness and ^{c}Specific surface area

Similarly, GO can be functionalized using different materials (see 9).

Table 9), such as with, tetraethylenepentamine (TEPA) [9], 3-aminopropyltriethoxysilane (APTES) [107], imidazole [108], *P*-phenylene diamine (PPD) and poly(thiophene-co-poly(methyl methacrylate) [56], dopamine [109], liquid crystalline perylenebisimide polyurethane (LCPBI) [110] and diaminodiphenyl sulphone (DDS) [18] as reducing agents and modifiers for GO to avoid agglomeration and improve adhesion between GO and epoxy. The λ of an epoxy on addition of 0.5

28

wt% TEPA functionalized GO increased from 0.35 to 0.71 W/(mK). The good adhesion observed (Figure 5 (b)) between the epoxy resin and GO-TEPA may also be attributed to the presence of the amine group covalently linked on the surface of GO, increasing the compatibility between epoxy and GO [9]. 1 wt% poly(thiophene) (PTh) and PPD grafted GO enhanced λ of an epoxy and a value of 1.24 W/(mK) at about 36 $^{\circ}$C was achieved. Similarly, λ was found to increase due to enhanced interactions between epoxy and nanofiller [55]. Other chemical groups have also been employed to functionalize GO, e.g., fullerene [111], silica [112, 113], $Al(OH)_3$ [114] and NH_2 [115]. However, the λ of NH_2 and $Al(OH)_3$ coated GO reinforced epoxy decreased compared to the neat GO filled epoxy. This can be attributed to the poor dispersion and wettability of $GO-NH_2$ or $GO-Al(OH)_3$ with the epoxy used. Several cracks and air gaps were present between the $GO-NH_2$ sheets and epoxy matrix due to the hydrophobic nature of the $GO-NH_2$ sheets. Such defects increased thermal resistance by phonon–phonon scattering, boundary scattering, and defect scattering [115] and, attenuate the λ of the epoxy composite. The λ of the composites depends on both the extent of 2D nanofiller dispersion and distribution in the epoxy matrix and the interfacial interactions between the matrix and filler. The addition of GO did not effectively improve the λ of the epoxy, which in this instance may be due to the modulus mismatch between the soft epoxy matrix and rigid unfilled GO that induces phonon scattering. Silica-coated graphene (S-graphene) sheets improved the λ of an epoxy by 72% on addition of 8 wt% S-graphene compared to neat epoxy [107]. The presence of Si nanoparticles can not only enhance interfacial interaction between graphene and the epoxy matrix, but also act as a buffer layer to alleviate the modulus mismatch and thus contribute to interfacial thermal conductance.
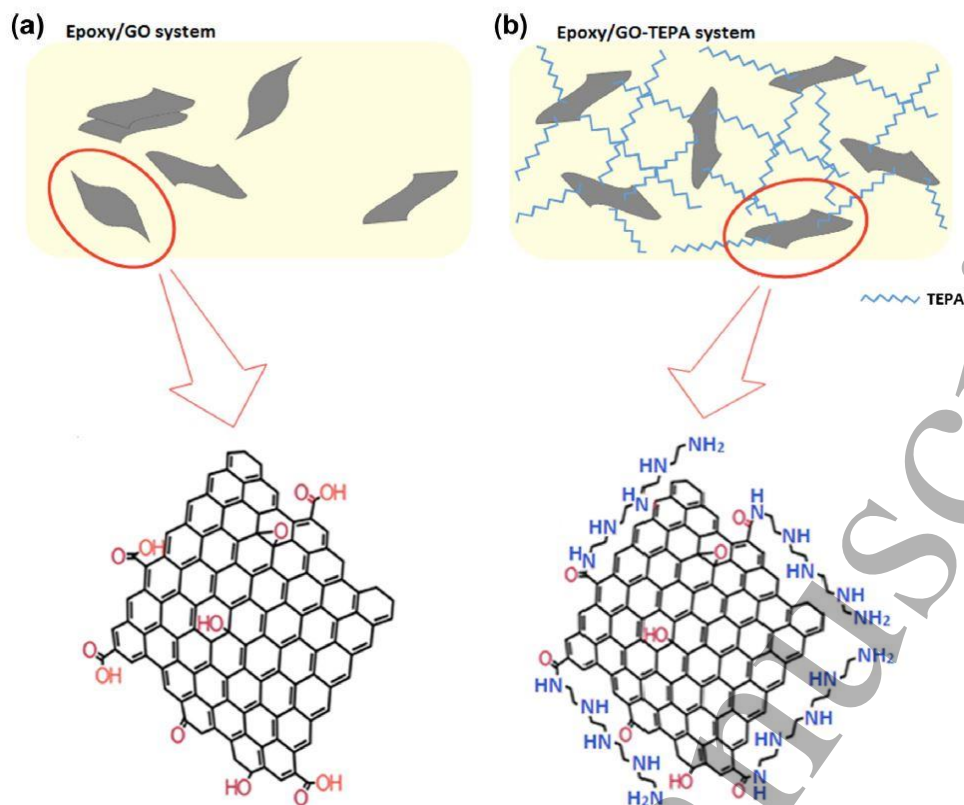
Figure 5. Schematic showing the interaction between an epoxy with (a) neat GO and (b) TEPA functionalized GO [9].

Table 9. Thermal conductivity (λ) of composites of functionalized GO and epoxy

Filler (mixing techniques)	λ (W/mK)	Epoxy type	Filler size and surface treatment	Reference
(1)0.5wt% TEPA-GO (2)0.5wt%raw-GO (mixing + 3-roll mill)	(1)0.35-0.71 (2)0.35-0.59 (laser flash)	DER331 (DOW) liquid DGEBA (TETA) hardener	GO size: a few hundred nanometres to a few micrometres, T:1.5 nm(1-3 layers), thin, transparent and wrinkled sheets TEPA functionalized GO	[9]
8wt% silica coated GO (ultrasonic mixing monomer)	0.173-0.3 (similar to hot wire method)	DGEBA (JY257) MeHHPA	T:10-20nm. functionalisation and reduction of GO with APTES, then coated with silica, smooth and compact surface	[107]
15phr GO (magnetic stirring)	0.26-0.37 (laser flash)	DGEBA-618 MTHPA	D: 200nm, dopamine was used as reducing agent and modifier for GO to avoid using a harmful reducing agent and agglomeration,	[109]

30

			improved adhesion between GO and epoxy.	
0.8wt% GO (ultrasonic + mixing)	0.22-0.29 (laser flash)	DGEBA (E51)	Imidazole grafted GO	[108]
0.5vol% DDS-GO (ultrasonic + mixing)	0.06-0.493 (laser flash)	618 epoxy resin	D:10-15μm, T:1-1.6nm (1-3layers), diaminodiphenyl sulphone (DDS) functionalized GO	[18]
30wt% Al$_2$O$_3$ + 0.3wt% LCPBI/ RGO (ultra-sonication + stirring)	0.16-0.329 (thermal diffusivity ASTM E1461)	DGEBA (E-51)	Corrugation and scrolling surface of RGO. liquid crystalline perylene-bisimide polyurethane (LCPBI) non-covalently functionalized reduced GO. Silane grafted Al$_2$O$_3$	[110]
0.36wt% MWCNTs + 49.64wt% GO (solution compounding)	Up to 4.4 (laser flash)	DGEBF	GNPs D:μm, T:4-5nm The polar functionality on the GO and MWCNTs were purified and functionalized with carboxylic acid functional groups	[116]
71wt% fullerene coated GO (solution blend)	0.3-0.66 laser flash	Epon862 EPI Cure-W	GO interlayer spacing 0.72nm, while nature graphite is 0.34nm. Fullerene coating reduce lattice λ by scattering phonons	[111]
1wt% silica coated thermally reduced GO (ultrasonic + mixing)	0.2-0.322 (laser flash)	BE188	GO-silica nanosheet sandwich made by sol-gel process, silica layer coated on the surface of GO, not wrinkled	[112]
1.5wt% GO (exfoliated into single layer) (stirring)	0.21-0.29 (DRL-II TC meter)	DGEBA DETDA	D:0.2-1 μm, T:1 nm nanosilica coated GO	[113]
20wt% GO (ultrasonic + mixing)	0.2-6.1 (laser flash)	n/a	3-10 layers, thermally reduced GO with less functional group	[117]

31

(1)80wt% Al_2O_3 + 10wt% GO (2) 80 wt% Al_2O_3 + 10wt% $Al(OH)_3$ coated GO (3-roll mill)	(1)0.2-3.6 (2)0.2-3.2 (laser flash)	DGEBA	T:50-150nm for $Al(OH)_3$ coated graphene oxide (not as good as raw GO)	[114]
(1) 3wt% NH_2-GO (2) 3wt% GO (sonication + mixing)	(1)0.188-0.311 (2)0.188-0.351 (laser flash)	DGEBA KUKDO DDM	GO better than GO-NH_2 for improved λ	[115]

^{a}Dimension (average diameter), ^{b} Thickness and ^{c}Specific surface area

5.4 Effect of filler alignment

Alignment is understood as a preferred orientation of a graphene in all three-dimensions in a sample which may result in a change in a specific property, such as when λ enhancement is desired in a preferred direction. The under-performance of GNPs in comparison with theoretical predictions originates from the high interfacial thermal resistance (ITR) between GNPs and the epoxy matrix [118-119]. Owing to the planar geometry of graphene(s), for thermal transport from graphene to polymer, ITR mainly occurs at the interface between the graphene basal plane and epoxy matrix, while the ITR at the graphene edge/matrix interface is considerably reduced. Thus, good alignment of GNPs in composites can substantially minimize ITR along the alignment direction, resulting in a significant enhancement in λ.

A facile approach was developed to align magnetically functionalized graphene nanosheets (M-GNSs) within an epoxy matrix [120]. M-GNSs were firstly synthesized by a modified polyol method with surface modification using Fe_3O_4 nanoparticles, and then incorporated into an epoxy under an externally applied magnetic field. Both good filler dispersion and a high degree of alignment were obtained in the composites treated with a magnetic field above 0.5T, verified by X-ray diffraction and polarized Raman spectra. The value of λ in the aligned direction of these composites with a 0.52 vol% filler content was 0.361 ± 0.018 W/(mK) an enhancement of $111 \pm 28\%$ and $48 \pm 16\%$, compared to that of neat epoxy (0.174 ± 0.014 W/(mK) and non-magnetically treated composites (0.252 ± 0.019

32

W/(mK), respectively. However, the employment of this method to align high loadings of M-GNSs (>10 vol% or more) is problematic, and current investigations show the λ of aligned 10 vol% M-GNS/epoxy composites is not much better than that of unaligned counterparts, due to the high viscosity of the matrix with increasing filler loading.

rGO nanosheets were prepared by a vacuum-assisted self-assembly method [121]. The basal planes of most rGO nano-sheets are nearly parallel and it displays an aligned laminated structure in the in-plane direction. Biphenyl mesogenic epoxy nanocomposites were obtained based on a mesogenic epoxy and rGO nanosheets via infiltration. Heat transfer channels in the in-plane direction were formed and the composite showed anisotropic thermal conductivity. In-plane and through-plane thermal conductivity of the composite was 1.3209 W /mK and 0.1725 W/mK containing 27.8 wt% rGO nanosheets, respectively.

5.5 Effect of addition of hybrid fillers

The addition of GNPs with other types of carbon nanofillers to epoxies, i.e. a hybrid filled system, shows great potential and could significantly broaden the applications of GNPs. Hybrid fillers are commonly used in thermally conductive composites, as a better thermally conductive network can be formed by using different fillers having different sizes and geometry. Hybrid filler systems can help to form large thermally conductive networks via bridging between different fillers and maximising filler packing density. Another advantage of a hybrid filler system is that it may help to significantly reduce the overall filler loading, thus reducing system viscosity, particular pertinent with regard epoxies.

5.5.1 Combining fillers with different sizes (μm and nm)

The λ of composites of epoxy, expanded graphite (EG, natural based graphite which has been exfoliated, calendared and sized, thickness: μm) and graphene oxide (GO, less than 3 layers, thickness: nm) in varying ratios has been measured [122]. Thermal characterisation showed unexpectedly high thermal conductivities at certain filler ratios. This phenomenon was exhibited by

samples with three different overall filler concentrations (EG+GO) of 7, 14, and 35 wt%. The highest λ of 42.4 W/(mK) (nearly 250 times the λ of unfilled epoxy) was seen for a sample with 30 wt% EG and 5 wt% GO when characterised using a dual-mode heat flow meter technique. This significant improvement in λ can be attributed to the lowering of the overall thermal interface resistance due to small amounts of GO improving the thermal contact between the primary micro-filler (EG).

Shetin *et al.* incorporated 16 vol% GNPs (15 μm lateral size and 10 nm thickness) and 1 vol% nano- boron nitride particles (110 nm lateral size) into an epoxy resin. The thermal conductivity of the composite increased from 0.2 W/mK (neat epoxy) to 4.72 W/mK [85].

5.5.2 Combining fillers with different shapes (1D and 2D)

CNTs can considerably improve heat transport in polymer composites as a result of their 1D structure, high λ and high aspect ratio [123-125]. The combination of 1D CNTs and 2D GNPs (see Table 10) leads to a synergistic effect in enhancement of λ of epoxies. Chang *et al.* prepared epoxy composites containing 1.525 wt% MWCNTs and 4.575 wt% GNPs [62]. The λ of the composites was increased from 0.23 to 0.89 W/(mK). The increased λ is ascribed to the formation of a more efficient percolating nanofiller network with reduced thermal interface resistances. The long and tortuous CNTs can bridge adjacent GNPs and inhibit their aggregation, resulting in an increased contact surface area between GNP-CNT structures and the polymer matrix.

Table 10. Thermal conductivity (λ) of composites of epoxy with GNPs and CNTs

Fillers(mixing techniques)	λ (W/(mK))	Epoxy type	Filler size [a,b] and surface treatment	Reference
7.5wt% GNPs+ 2.5wt% SWCNTs (ultrasonic + stirring with acetone)	0.2-1.75 (steady state heat flow)	DGEBF, EPON862	GNPs D[a]:350nm, T[b]:2nm	[126]
1.525wt% MWCNTs + 4.575wt% GNPs	0.23-0.89 (laser flash)	DGEBA (5000-6000 cps)	D:550nm, T: 8 nm, SSA[c]:100 m^2/g scCO$_2$-assisted mixing to prepare	[63]

34

(scCO$_2$-assisted magnetic stirring)			graphene /CNTs/epoxy composites	
0.9wt% GNPs + 0.1wt% MWCNTs (ultra-sonication + high shear)	0.13-0.32 (hot disk)	EPON 128 with curing agent (POP-D400)	GNPs D: sub-micrometre to 100μm, T:1-15nm Glycidyl methacrylate (GMA) grafted MWCNTs	[127]
20wt% CNTs directly grown on the GNP (shear mixing to form a suspension)	Up to 2.41 through plane (laser flash)	KFR-120 KFH-150	CNTs were synthesized on the GNP support via chemical vapour deposition process	[128]
0.36wt% MWCNTs + 49.64wt% GNPs (solution compounding)	Up to 4.4 (laser flash)	DGEBF	GNPs D: μm, T: 4-5nm. polar functionality on the GO (GNPs) and MWCNTs purified and functionalized with COOH	[116]
1wt% MWCNTs + 1wt% GNPs (3-roll mill, gap 5μm, 270rpm)	0.24-0.34 (DRL-III TC meter)	CYD-128	GNPs D: hundreds of nanometres to tens of micrometres T:2-4 nm(8 layers)	[74]
17wt%GNPs + 3%CNTs (shear mixer)	Up to 4.7 in plane Up to 2.5 through plane (laser flash)	DGEBA (KFR-120) KFH-150	D: 25μm, T: 6-8nm, SSA:120-150 m^2/g. Fe-Co coated GNPs by electro-less plating, via bimetallic nanoparticle decoration on GNP surface and subsequent CVD	[99]
1wt%CNTs+0.01 wt%GNPs (in-situ polymerisation)	2.6-11.8 (hot disk)	Silver filled conductive epoxy resin	Double-walled CNTs functionalized with COOH and NH$_2$ terminal groups diameter: 1-4 nm and lengths: 1−5 μm	[129]

[a]Dimension (average diameter), [b] Thickness and [c]Specific surface area.

5.5.3 Combining 2D graphitic fillers with ceramic materials

In practice, polymeric packaging materials for electronic devices require high λ, low coefficient of thermal expansion, low dielectric permittivity and good electrical insulation. There has

35

been much published (see Table 11) to address the issue of heat dissipation of epoxy resins for electronic packaging applications by adding ceramic, metal, or other thermal conductive fillers such as graphite and its derivatives. Accordingly, various dielectric composite systems have been investigated to achieve high λ using thermally-conductive but electrical insulating fillers such as silica (SiO_2), aluminium oxide (Al_2O_3), silicon carbide (SiC) and aluminium nitride (AlN). These fillers can also be used in hybrid filled systems with GNPs to enhance λ. The main mechanism is to build a thermally conductive interconnected path or network in the epoxy matrix by adding fillers with high λ. For example, the addition of 50 vol% Al_2O_3 fibres and 2 vol% GNPs enhanced the λ of an epoxy from 0.2 to 1.62 W/(mK) [130].

Table 11. Thermal conductivity (λ) of composites of an epoxy with GNPs and ceramic materials

Fillers (mixing technique)	λ (W/mK)	Epoxy type	Filler size	Reference
2vol% GNPs + 50vol% Al_2O_3 fibres (sonication with acetone + stirring)	0.2-1.62 (laser flash)	E-51	D: 1-20 μm, T: 5-15 nm. Al_2O_3 were prepared by sol-gel	[130]
(1) 45wt% Al_2O_3 + 5wt% AlN-CNTs (2) 45wt% Al_2O_3 + 5wt% AlN-graphene (solution blending and casting method)	(1)0.2-0.55 (2)0.2-0.57 (hot disk)	DGEBA Anhydride	$D_{(CNTs)}$: 10-30nm, CNTs length:10-15μm, $D(Al_2O_3)$:5μm	[132]
68wt% Al_2O_3 + 7wt% GNPs + 5wt%$Mg(OH)_2$ (solution compounding, casting and curing)	0.2-2.2 (ECO HC-110 thermal meter)	DGEBA MHHPA	Silane grafted GNPs, synergistic effect for flame retardancy	[103]
(1)80wt% Al_2O_3 + 10wt% GO (2) 80wt% Al_2O_3 + 10wt%Al(OH)$_3$ coated GO (3-roll mill)	(1)0.2-3.6 (2)0.2-3.2 (laser flash)	DGEBA	T:50-150nm for $Al(OH)_3$ coated GO (not as good as neat GO)	[114]
30wt% Al_2O_3 + 0.3wt% LCPBI/reduced GO	0.16-0.329 (thermal	E-51 DGEBA	Corrugation and scrolling surface of RGO. LCPBI non-	[110]

36

(ultra-sonication + stirring)	diffusivity)		covalently functionalized reduced GO. Silane grafted Al_2O_3	
(1) 8wt% GO (2) 70wt% AlN (3) 6wt% GO + 50wt% AlN (ultra-sonication + stirring)	(1)0.19-1.22 (2)0.19-2.24 (3)0.19-2.77 (Hot disk)	DGEBA MeHHPA DMP	GO with high aspect ratio Most GO is in single layer	[131]
7wt% (GNPs+SiC) (ultra-sonication with acetone)	0.2-0.33 (laser flash)	E51 Diethylene triamine	Iron-catalyzed heat-treatment process to grow SiC on GNPs	[133]

[a] Dimension (average diameter), [b] Thickness and [c] Specific surface area.

6. Concluding remarks and perspectives

Heat management is critical for many applications, such as for electronic device design, electric motors and generators, heat exchangers in power generation, aerospace and automotive components and tooling. Metallic materials are widely used as heat dissipation materials, but high thermally conductive polymer based composites, such as those based on epoxies are emerging as alternatives, due to their lightweight, corrosion resistance, ease of processing (relative to metals) and low manufacturing cost.

The outstanding λ of 2D graphitic materials makes them promising candidates to obtain highly thermally conductive polymer based composites. Different types of 2D graphitic materials, including natural graphite (NG), expanded graphite (EG), graphite nanoplatelets (GNPs) and graphene oxide (GO) have been studied. The λ of the resultant epoxy composites depends on 2D filler structure, morphology, geometry and alignment in the polymer matrix. Various processing techniques such as *in-situ* polymerisation, solution blending and milling have been explored for preparation of composites of epoxies and 2D graphitic materials. To achieve a better dispersion and distribution of graphitic materials in the epoxy matrix, a combination of different processing techniques or hybrid

37

fillers are necessary. Strategies to improve thermal conductivity of composites with epoxy and 2D graphitic fillers are summarised in Figure 6.
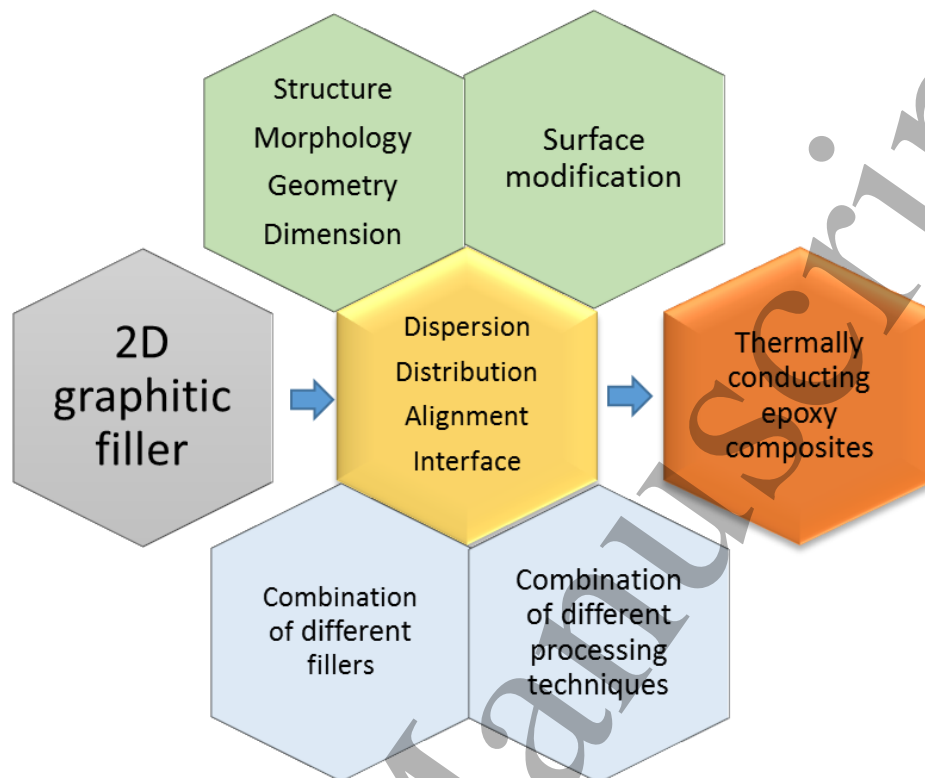

Figure 6. Schematic diagram showing the possible strategies to improve the thermal conductivity of composites of epoxy on addition of 2D graphitic fillers

Several technical challenges remain to be addressed in order to enhance the thermal conductivity of epoxy resins. In particular, the interface between the 2D filler and epoxy resin combined with an understanding of the factors that control filler dispersion and distribution in the polymer matrix are critical to achieving enhanced thermally conducting epoxy resins. Fundamentally, phonon scattering at the interface between the 2D filler and the epoxy (any polymer) matrix must be addressed, otherwise modest and technologically irrelevant increases in λ will continue to be reported. Conservatively, at least a 50 to 100 fold increase in λ of the epoxy is required to meet even basic thermal management applications in practice. Furthermore, effective dispersion and distribution of the 2D filler in the epoxy matrix using scalable and industrially relevant processes is a non-trivial matter. Strategies to address these challenges require further more innovative approaches. These include, but are not limited to;

38

(1) Filler selection - hybrid filled systems: addition of GNPs or GO with micron scale fillers (e.g. expanded graphite (EG) or natural graphite (NG)) can yield enhancements in λ. This could be further extended to include 2D graphitic fillers with 0D or 1D carbon or 0D, 1D or 2D thermally conductive inorganic materials, e.g. boron nitride to produce 'multi-generation' filled epoxies. The concept is to produce an interconnected filler network across the length scales minimising phonon scattering.

(2) Mixing/processing: it appears that a combination of different techniques may be required to facilitate effective dispersion and distribution of the 2D fillers in the epoxy precursor or matrix. By way of example, mechanical mixing followed by 3-roll milling or calendaring techniques could be used. Wrinkling and twisting of the graphitic sheets/platelets are often observed during high shear mixing, which is detrimental to thermal conduction. The rigidity of the graphitic platelets can be overcome by doping the graphitic sheets/platelets with hetero-elements or metal oxides.

(3) Surface treatment or introduction of crosslinks between the 2D filler and matrix: coating the surface of the platelets with, (a) metals, such as Ag coated 2D graphitic materials or with (b) a polymer (containing epoxide groups), such as with an epoxy-based monomer, would facilitate matrix-filler interactions and thus reduce the thermal resistance at the interface. Similarly, the introduction of a critically minimum density of crosslinking between neighbouring 2D filler sheets/platelets as well as the sheets/platelets and epoxy matrix will significantly reduce interfacial thermal resistance (ITR) and result in increased phonon conduction. However, the density of crosslinks would need to be balanced with other properties such as fracture toughness of the composites.

The goal of producing polymeric materials with high thermal conductivity, even anything close to that of metals (typically between 70 – 300 W/mK) by the addition of 2D graphitic materials remains a major scientific challenge, but one which if solved could revolutionize materials science and thermal management across a plethora of technologies. The limited understanding of phonon scattering at the polymer-2D filler interface and the lack of systematic studies with regard to the factors that control 2D filler dispersion in epoxy (polymer) matrices must be addressed.

39

Acknowledgements

References

[1]   Dodiuk H and Goodman S H 2013 *Handbook of Thermoset Plastics* (San Diego: William Andrew) p 191-200.

[2]   Wong C 1993 *Polymers for Electronic & Photonic Application* (Massachusetts: Academic Press) p 287-290.

[3]   Chen H, Ginzburg V V, Yang J, Yang Y, Liu W, Huang Y, Du L and Chen B 2016 Thermal conductivity of polymer-based composites: Fundamentals and applications *Prog. Polym. Sci.* **59** 41-85.

[4]   Sato K, Hitomi H, Takashi S, Yuji H, Hiromi N, Hideaki N, Kenshi M and Koji W 2010 Thermally conductive composite films of hexagonal boron nitride and polyimide with affinity-enhanced interfaces *J. Mater. Chem.* **20**(14) 2749-52.

[5]   Zhou W, Qi S, An Q, Zhao H and Liu N 2007 Thermal conductivity of boron nitride reinforced polyethylene composites *Mater. Res. Bull.* **42**(10) 1863-73.

[6]   Harada M, Hamaura N, Ochi M and Agari Y 2013 Thermal conductivity of liquid crystalline epoxy/BN filler composites having ordered network structure. *Compos. Part B: Eng.* **55** 306-313.

[7]   May C 1987 *Epoxy Resins: Chemistry and Technology* (Florida: CRC press)p 285-300.

[8]   Moriche R, Prolongo S G, Sanchez M, Jimenez-Suarez A, Chamizo F J and Urena A 2016 Thermal conductivity and lap shear strength of GNP/epoxy nanocomposites adhesives *Int. J. Adhes. Adhes.* **68** 407-10.

[9]   Ribeiro H, Silva W, Neves J, Calado H, Paniago R, Seara L and Camarano D 2015 Multifunctional nanocomposites based on tetraethylenepentamine-modified graphene oxide/epoxy *Polym. Test.* **43** 182-92.

[10]   Yu A, Ramesh P, Itkis M, Bekyarova E and Haddon R 2007 Graphite nanoplatelet-epoxy composite thermal interface materials *J. Phys.Chem. C* **111**(21) 7565-9.

[11]   Lee, H. and Neville K 1967 *Handbook of Epoxy Resins* (New York: McGraw-Hill) p 133.

[12]   Garrett, K. and Rosenberg H 1974 The thermal conductivity of epoxy-resin/powder composite materials *J. Phys. D: Appl. Phys.* **7**(9) 1247.

[13]   Chung S L and Lin J S 2016 Thermal conductivity of epoxy resin composites filled with combustion synthesized h-BN particles *Molecular* **21**(5) 670.

[14]   Wang Y, Yu J, Dai W, Song Y, Wang D, Zeng L and Jiang N 2015 Enhanced thermal and electrical properties of epoxy composites reinforced with graphene nano-platelets *Polym. Compos.* **36**(3) 556-65.

[15]   Tang X, Zhou Y, and Peng M 2016 Green preparation of epoxy/graphene oxide nanocomposites using a glycidylamine epoxy resin as the surface modifier and phase transfer agent of graphene oxide *ACS Appl. Mater. Interfaces* **8**(3) 1854-66.

[16]   Rohsenow W M, Hartnett J P, and Cho Y I 1998 *Handbook of Heat Transfer* vol. 3 (New York: McGraw-Hill).

[17]   Agari Y and Ueda A 1997 Thermal diffusivity and conductivity of PMMA/PC blends *Polym.* **38**(4) 801-7.

[18]   Hu Y, Shen J, Li N, Ma H, Shi M, Yan B, Huang W, Wang W and Ye M 2010 Comparison of the thermal properties between composites reinforced by raw and amino-functionalized carbon materials *Compos. Sci. Technol.* **70**(15) 2176-82.

[19]   Chatterjee S, Wang J W, Kuo W S, Tai N H, Salzmann C, Li W L, Hollertz R, Nuesch F A and Chu B T T 2012 Mechanical reinforcement and thermal conductivity in expanded graphene nano-platelets reinforced epoxy composites *Chem. Phys. Lett.* **531** 6-10.

[20]   Giang T and Kim J 2016 Effect of liquid-crystalline epoxy backbone structure on thermal conductivity of epoxyc alumina composites *J. Electron. Mater.* **34**(4)1-10.

[21]   Wypych G 2000 *Handbook of Fillers: Physical Properties of Fillers and Filled Materials* (Toronto: ChemTech Publishing)

[22]   Wang S, Cheng Y, Wang R, Sun J and Gao L 2014 Highly thermal conductive copper nanowire composites with ultralow loading: Toward applications as thermal interface materials *ACS Appl. Mater. Interfaces* **6**(9) 6481-86.

[23]   Bjorneklett A, Halbo L and Kristiansen H 1992 Thermal conductivity of epoxy adhesives filled with silver particles *Int. J. Adhes. Adhes.* **12**(2) 99-104.

[24]   Kim P, Shi L, Majumdar A and McEuen P L 2001 Thermal transport measurements of individual multiwalled nanotubes *Phys. Rev. Lett.* **87**(21) 215502.

[25]   Sauvajol J L, Anglaret E, Rols S and Alvarez L 2002 Phonons in single wall carbon nanotube bundles *Carbon* **40**(10) 1697-1714.

[26]   MInus M and Kumar S 2005 The processing, properties, and structure of carbon fibers *JOM* **57**(2) 52-8.

[27]   Endo M 1988 Structure of mesophase pitch-based carbon fibres *J. Mater. Sci.* **23**(2) 598-605.

[28]   Stankovich S, Dikin D A, Dommett G, Kohlhaas K M, Zimney E J, Stach E A, Piner R D, Nguyen S T and Ruoff R S 2006 Graphene-based composite materials *Nature* **442**(7100) 282-6.

[29]   Smalc M, Shives G, Chen G, Guggari S, Norley J and Reynolds R A 2005 Thermal performance of natural graphite heat spreaders *in ASME 2005 Pacific Rim Technical Conference and Exhibition on Integration and Packaging of MEMS, NEMS, and Electronic Systems collocated with the ASME 2005 Heat Transfer Summer Conference* San Francisco.

[30]   Ngo I L, Jeon S and Byon C 2016 Thermal conductivity of transparent and flexible polymers containing fillers: A literature review *Int. J. Heat Mass Transfer* **98** 219-26.

[31]   Kume S, Yamada I and Watari K 2009 High‑Thermal‑Conductivity AlN filler for polymer/ceramics composites *J. Am. Ceram. Soc.* **92**(s1) s153-s156.

[32]   Akishin G, Turnaev S, Vaispapir V, Gorbunova M, Makurin Y, Kiiko V and Ivanovskii 2009 Thermal conductivity of beryllium oxide ceramic *Refract. Ind. Ceram.* **50**(6) 465-8.

[33]   Li T L and Hsu S 2010 Enhanced thermal conductivity of polyimide films via a hybrid of micro-and nano-sized boron nitride *J. Phys. Chem. B* **114**(20) 6825-29.

[34]   Kelly B T 1981 *Physics of Graphite (*London: Applied Science)

[35]   Boehm H P, Setton R and Stumpp E 1994 Nomenclature and terminology of graphite intercalation compounds *Pure Appl. Chem.* **66** 1893-1901.

[36]   Dresselhaus M and Dresselhaus G 1981 Intercalation compounds of graphite *Adv. Phys.* **30**(2) 139-326.

[37]   Stevens R E, Ross S and Wesson S P 1973 Exfoliated graphite from the intercalate with ferric chloride *Carbon* **11**(5) 525-530.

[38]   Yoshida A, Hishiyama Y and Inagaki M 1991 Exfoliated graphite from various intercalation compounds *Carbon* **29**(8) 1227-31.

[39]   Chen G H, Wu D, Weng W, He B and Yan W 2001 Preparation of polystyrene–graphite conducting nanocomposites via intercalation polymerization *Polym. Int.* **50**(9) 980-5.

[40]   Sengupta R, Bhattacharya M, Bandyopadhyay S and Bhowmick A 2011 A review on the mechanical and electrical properties of graphite and modified graphite reinforced polymer composites *Prog. Polym. Sci*. **36**(5) 638-70.

[41]   Viculis L M, Mack J J and Kaner R B 2003 A chemical route to carbon nanoscroll *Science* **299**: 1361.

[42]   Rafiee M A, Rafieet J, Wang Z, Song H, Yu Z and Koratkar N 2009 Enhanced mechanical properties of nanocomposites at low graphene content *ACS Nano* **3**(12) 3884-90.

[43]   Jang B Z and Zhamu Z 2008 Processing of nanographene platelets (NGPs) and NGP nanocomposites: a review *J. Mater. Sci*. **43**(15) 5092-101.

[44]   Jacob George J, Bandyopadhyay A and Bhowmick A K 2008 New generation layered nanocomposites derived from ethylene‑co‑vinyl acetate and naturally occurring graphite *J. Appl. Polym. Sci.* **108**(3) 1603-16.

[45]   Hummers Jr W S and Offeman R E 1958 Preparation of graphitic oxide *J. Am. Chem. Soc.* **80**(6) 1339.

[46]   Park S and Ruoff R S 2009 Chemical methods for the production of graphenes *Nat. Nanotechnol*. **4**(4) 217-24.

[47]   Schniepp H C, Li J, McAllister M, Sai H, Herrera-Alonso M, Adamson D, Prud'homme R, Car R, Saville and Aksay I 2006 Functionalized single graphene sheets derived from splitting graphite oxide *J. Phys. Chem. B* **110**(17) 8535-39.

[48]   McAllister M J *et al.* 2007 Single sheet functionalized graphene by oxidation and thermal expansion of graphite *Chem. Mater.* **19**(18) 4396-404.

[49] Renteria J D et al. 2015 Strongly anisotropic thermal conductivity of free-standing reduced graphene oxide films annealed at high temperature Adv. Funct. Mater **25**, 4664–4672.

[50]   Zheng W and Wong S C 2003 Electrical conductivity and dielectric properties of PMMA/expanded graphite composites *Compos. Sci. Technol.* **63**(2) 225-35.

[51]   Singh E and Nalwa H S 2015 Stability of graphene-based heterojunction solar cells *RSC Adv.* **5**(90) 73575-600.

[52]   Balandin A A 2011 Thermal properties of graphene and nanostructured carbon materials *Nat. Mater.* **10**(8) 569-81.

[53]   Mahanta NK and Abramson AR 2012 Thermal conductivity of graphene and graphene oxide nanoplatelets *Thermal and Thermomechanical Phenomena in Electronic Systems (ITherm), 13th IEEE Intersociety Conference* San Diego.

[54]   Eksik O, Bartolucci S, Gupta T, Fard H, Borca-Tasciuc T and Koratkar N 2016 A novel approach to enhance the thermal conductivity of epoxy nanocomposites using graphene core-shell additives *Carbon* **101** 239-44.

[55]   Fu Y, He Z, Mo D and Lu S 2014 Thermal conductivity enhancement with different fillers for epoxy resin adhesives *Appl. Therm. Eng.* **66**(1) 493-8.

[56]   Rahim S, Ayesha K, Bakhtiar M and Khan M 2016 Investigation on thermal conductivity and physical properties of polythiophene/p-phenylenediamine-graphene oxide and polythiophene-co-poly(methyl methacrylate)/p-phenylenediamine graphene oxide composites *Compos. Interface* **23**(9) 887-99.

[57]   Min C, Yu D, Cao J, Wang G and Feng L 2013 A graphite nanoplatelet/epoxy composite with high dielectric constant and high thermal conductivity *Carbon* **55** 116-25.

[58]   Huang X, Zhi C and Jiang P 2012 Toward effective synergetic effects from graphene nano-platelets and carbon nanotubes on thermal conductivity of ultrahigh volume fraction nanocarbon epoxy composites *J. Phys. Chem.* **116**(44) 23812-20.

[59]   Gao J, Yu J, Wu X, Rao B, Song L, He Z and Lu S 2015 Enhanced thermal properties for epoxy composites with a three-dimensional graphene oxide filler *Fiber. Polym.* **16**(12) 2617-26.

[60]   Czichos H, Saito T and Smith L 2006 *Springer Handbook of Materials Measurement Methods*. Vol. 978 (Heidelberg: Springer Berlin)

[61]   Solorzano E, Rodriguez‐Perez M and Saja J 2008 Thermal conductivity of cellular metals measured by the transient plane sour method *Adv. Eng. Mater.* **10**(4) 371-7.

[62]   Zhou T, Koga H, Nogi M, Sugahara T, Nagao S, Nge T T, Suganuma K, Cui H W, Liu F and Nishina Y 2015 Targeted kinetic strategy for improving the thermal conductivity of epoxy composite containing percolating multi-layer graphene oxide chains *Express Polym. Lett.* **9**(7) 608-23.

[63]   Chang H P, Liu H C and Tan C S 2015 Using supercritical CO_2/assisted mixing to prepare graphene/carbon nanotube/epoxy nanocomposites *Polymer* **75** 125-33.

[64]   Veca L M, Meziani M, Wang W, Wang X, Lu F, Zhang P, Lin Y, Fee R, Connell J and Sun Y 2009 Carbon nano-sheets for polymeric nanocomposites with high thermal conductivity *Adv. Mater.* **21**(20) 2088-92.

[65]   Tang B, Hu G, Gao H and Hai L 2015 Application of graphene as filler to improve thermal transport property of epoxy resin for thermal interface materials *Int. J. Heat Mass Transfer* **85** 420-29.

[66]   Xie F, Qi S H and Wu D 2016 A facile strategy for the reduction of graphene oxide and its effect on thermal conductivity of epoxy based composites *Express Polym. Lett.* **10**(6) 470-78.

[67]   Teng C, Ma C, Lu C, Yang S, Lee S, Hsiao M, Yen M, Chiou K and Lee T 2011 Thermal conductivity and structure of non-covalent functionalized graphene/epoxy composites *Carbon* **49**(15) 5107-16.

[68]   Tien D, Park J, Han S and Shin K 2011 Electrical and thermal conductivities of stycast 1266 epoxy/graphite composites *J. Korean Phys. Soc.* **59**(4) 2760-4.

[69]   Serena Saw W P and Mariatti M 2012 Properties of synthetic diamond and graphene nanoplatelet-filled epoxy thin film composites for electronic applications *J. Mater. Sci. Mater. Electron* **23**(4) 817-24.

[70]   Yan H, Tang Y, Long W and Li Y 2014 Enhanced thermal conductivity in polymer composites with aligned graphene nano-sheets *J. Mater. Sci.* **49**(15) 5256-64.

[71]   Kostagiannakopoulou C, Fiamegkou E, Sotiriadis G and Kostopoulos V 2016 Thermal conductivity of carbon nanoreinforced epoxy composites *J. Nanomater.* **2016**.

[72]   Zakaria M R, Abdul Kudus M H, Md. Akil H and Mohd Thirmizir M Z 2017 Comparative study of graphene nanoparticle and multiwall carbon nanotube filled epoxy nanocomposites based on mechanical, thermal and dielectric properties *Compos. Part B: Eng.* **119** 57-66.

[73]   Guo W and Chen G 2014 Fabrication of graphene/epoxy resin composites with much enhanced thermal conductivity via ball milling technique *J. Appl. Polym. Sci.* **131**(15) 40565-70.

[74]   He Z, Zhang X, Chen M, Li M, Gu Y, Zhang Z and Li Q 2013 Effect of the filler structure of carbon nanomaterials on the electrical, thermal, and rheological properties of epoxy composites *J. Appl. Polym. Sci.* **129**(6) 3366-72.

[75]   Hsu C, Hsu M, Chang K, Lai M, Liu P, Chuang T, Yeh J and Liu W 2014 Physical study of room-temperature-cured epoxy/thermally reduced graphene oxides with various contents of oxygen-containing groups *Polym. Int.* **63**(10) 1765-70.

[76]   Li Y, Zhang H, Porwal H, Huang Z, Bilotti E and Peijs T 2017 Mechanical, electrical and thermal properties of in-situ exfoliated graphene/epoxy nanocomposites *Compos. Part A* **95** 229-36.

[77]   Wang F, Drzal L, Qin Y and Huang Z 2015 Mechanical properties and thermal conductivity of graphene nanoplatelet/epoxy composites *J. Mater. Sci.* **50**(3) 1082-93.

[78]   Prolongo S G, Moriche R, Jimenez-Suarez A, Sanchez M and Urena A 2014 Advantages and disadvantages of the addition of graphene nano-platelets to epoxy resins *Eur. Polym. J.* **61** 206-14.

[79]   Chatterjee S, Nafezarefi F, Tai N H, Schlagenhaul L, Nuesch F A and Chu B 2012 Size and synergy effects of nano-filler hybrids including graphene nano-platelets and carbon nanotubes in mechanical properties of epoxy composites *Carbon* **50**(15) 5380-6.

[80]   Wang F, Drzal L, Qin Y and Huang Z 2016 Enhancement of fracture toughness, mechanical and thermal properties of rubber/epoxy composites by incorporation of graphene nano-platelets *Compos. Part A: Appl. Sci. Manuf.* **87** 10-22.

[81]   Ahmadi-Moghadam B and Taheri F 2014 Effect of processing parameters on the structure and multi-functional performance of epoxy/GNP-nanocomposites *J. Mater. Sci.* **49**(18) 6180-90.

[82]   Esposito Corcione C and Maffezzoli A 2013 Transport properties of graphite/epoxy composites: Thermal, permeability and dielectric characterisation *Polym. Test.* **32**(5) 880-8.

[83]   Fu Y, He Z, Mo D and Lu S 2014 Thermal conductivity enhancement of epoxy adhesive using graphene sheets as additives *Int. J. Therm. Sci.* **86** 276-83.

[84]   Shtein M, Nadiv R, Buzaglo M, Kahil K and Regev O 2015 Thermally conductive graphene-polymer composites: size, percolation, and synergy effects *Chem. Mater.* **27**(6) 2100-6.

[85]   Shtein M, Nadiv R, Buzaglo M and Regev O 2015 Graphene-based hybrid composites for efficient thermal management of electronic devices *ACS Appl. Mater. Interfaces* **7**(42) 23725-30.

[86]   Zhou T, Liu F, Suganuma K and Nagao S 2016 Use of graphene oxide in achieving high overall thermal properties of polymer for printed electronics *RSC Adv.* **6**(25) 20621-28.

[87]   Kim HS, Kim JH, Kim WY, Lee HS, Kim SY and Khil MS 2017 Volume control of expanded graphite based on inductively coupled plasma and enhanced thermal conductivity of epoxy composite by formation of the filler network *Carbon 119* 40-6.

[88]   Shahil K M and Balandin A A 2012 Graphene-multilayer graphene nanocomposites as highly efficient thermal interface materials *Nano Lett.* **12**(2) 861-67.

[89]   Chu K, Li. W and Dong H 2013 Role of graphene waviness on the thermal conductivity of graphene composites *Appl. Phys. A: Mater. Sci. Process.* **111**(1) 221-5.

[90]   Sha J, Li G, Chen X, Xia P, Luo R, Yang S, Chen T, Ma Y and Xie L 2016 Simultaneous ultra-sonication assisted internal mixing to prepare MWCNTs filled epoxy composites with increased strength and thermal conductivity *Polym. Compos.* **37**(3) 870-80.

[91]   Gojny F H, Nastalczyk J, Roslaniec Z and Schulte K 2003 Surface modified multi-walled carbon nanotubes in CNT/epoxy-composites *Chem. Phys. Lett.* **370**(5) 820-24.

[92]   Alam A, Wan C and McNally T 2016 Surface amination of carbon nanoparticles for modification of epoxy resin: plasma treatment vs wet-chemistry approach *Eur. Polym. J.* **87** 422-48

[93]   Wang F, Drzal L, Qin Y and Huang Z 2016 Effects of functionalized graphene nano-platelets on the morphology and properties of epoxy resins *High Perform. Polym.* **28**(5) 525-36.

[94]   Gu J, Yang X, Lv Z, Li N, Liang C and Zhang Q 2016 Functionalized graphite nano-platelets/epoxy resin nanocomposites with high thermal conductivity *Int. J. Heat Mass Transfer* **92** 15-22.

[95]   Gu J, Liang C, Zhao X, Gan B, Qiu H, Guo Y, Yang X, Zhang Q and Wang D 2017 Highly thermally conductive flame-retardant epoxy nanocomposites with reduced ignitability and excellent electrical conductivities *Compos. Sci. Technol.* **139** 83-9.

[96]   Ma Q, Luo J, Chen Y, Wei W, Liu R and Liu X 2015 Reactive copolymer functionalized graphene sheet for enhanced mechanical and thermal properties of epoxy composites *J. Polym. Sci. A Polym. Chem.* **53**(23) 2776-85.

[97]   Zong P, Fu J, Chen L, Yin J, Dong X, Yuan S, Shi L and Deng W 2016 Effect of aminopropylisobutyl polyhedral oligomeric silsesquioxane functionalized graphene on the thermal conductivity and electrical insulation properties of epoxy composites *RSC Adv.* **6**(13) 10498-506.

[98]   Chen L, Zhao P, Xie H and Yu W 2016 Thermal properties of epoxy resin based thermal interfacial materials by filling Ag nano-particle-decorated graphene nano-sheets *Compos. Sci. Technol.* **125** 17-21.

[99]   Park J S, An Y J, Shin K, Han J H and Lee C S 2015 Enhanced thermal conductivity of epoxy/three-dimensional carbon hybrid filler composites for effective heat dissipation *RSC Adv.* **5**(58) 46989-96.

[100]   Sun R, Yao H, Zhang H-B, Li Y, Mai Y-W and Yu Z-Z 2016 Decoration of defect-free graphene nanoplatelets with alumina for thermally conductive and electrically insulating epoxy composites *Compos. Sci. Technol.* **137** 16-23.

[101]   Kim J, Yim B, Kim J and Kim J 2012 The effects of functionalized graphene nano-sheets on the thermal and mechanical properties of epoxy composites for anisotropic conductive adhesives (ACAs) *Microelectron. Reliab.* **52**(3) 595-602.

[102]   Cao L, Liu X, Na H, Wu Y, Zheng W and Zhu J 2013 How a bio-based epoxy monomer enhanced the properties of diglycidyl ether of bisphenol A (DGEBA)/graphene composites *J. Mater. Chem. A* **1**(16) 5081-8.

[103]   Guan F, Gui C, Zhang H, Jiang Z, Jiang Y and Yu Z 2016 Enhanced thermal conductivity and satisfactory flame retardancy of epoxy/alumina composites by combination with graphene nano-platelets and magnesium hydroxide *Compos. Part B: Eng.* **98** 134-140.

[104]   Song S H, Park K H, Kim B H, Choi Y W, Jun G H, Lee D J, Kong B S, Paik K W and Jeon S 2013 Enhanced thermal conductivity of epoxy-graphene composites by using non-oxidized graphene flakes with non-covalent functionalisation *Adv. Mater.* **25**(5) 732-7.

[105]   Chiang T H, Liu C Y and Lin Y C 2015 The effect of an anhydride curing agent, an accelerant, and non-ionic surfactants on the electrical resistivity of graphene/epoxy composites *J. Appl. Polym. Sci.* **132**(20).

[106]   Zhao S, Chang H, Chen S, Cui J and Yan Y 2016 High-performance and multifunctional epoxy composites filled with epoxide-functionalized graphene *Eur. Polym. J.* **84** 300-12

[107]   Pu X, Zhang H, Li X, Gui C and Yu Z 2014 Thermally conductive and electrically insulating epoxy nanocomposites with silica-coated graphene *RSC Adv.* **4**(29) 15297-303.

[108]   Lei L, Shan J, Hu J, Liu X, Zhao J and Tong Z 2016 Co-curing effect of imidazole grafting graphene oxide synthesized by one-pot method to reinforce epoxy nanocomposites *Compos.Sci. Technol* **128** 161-8.

[109]   Hu X, Qi R, Zhu J, Lu J, Luo Y, Jin J and Jiang P 2014 Preparation and properties of dopamine reduced graphene oxide and its composites of epoxy *J. Appl. Polym. Sci.* **131**(2) 39754-64.

[110]   Zeng C, Lu S, Song L, Xiao X, Gao J, Pan L, He Z and Yu J 2015 Enhanced thermal properties in a hybrid graphene-alumina filler for epoxy composites *RSC Adv*. **5**(45) 35773-82.

[111]   Kun Z, Yue Z and Shiren W 2013 Effectively decoupling electrical and thermal conductivity of polymer composites *Carbon* **65** 105-111.

[112]   Hsiao M, Ma C, Chiang J, Ho K, Chou T, Xie X, Tsai C, Chang L and Hsieh C 2013 Thermally conductive and electrically insulating epoxy nanocomposites with thermally reduced graphene oxide-silica hybrid nano-sheets *Nanoscale* **5**(13) 5863-71.

[113]   Wang R, Zhuo D, Weng Z, Wu L, Cheng X, Zhou Y, Wang J and Xuan B 2015 A novel nanosilica/graphene oxide hybrid and its flame retarding epoxy resin with simultaneously improved mechanical, thermal conductivity, and dielectric properties *J. Mater. Chem. A* **3**(18) 9826-36.

[114]   Heo Y, Im H, Kim J and Kim J 2012 The influence of Al(OH)$_3$-coated graphene oxide on improved thermal conductivity and maintained electrical resistivity of Al$_2$O$_3$/epoxy composites *J. Nanopart. Res*. **14**(10) 1-10.

[115]   Yim B S, Kim K, Kim J and Kim J M 2016 Influence of functionalized graphene on the electrical, mechanical, and thermal properties of solderable isotropic conductive adhesives *J. Mater. Sci. Mater. Electron.* **27**(5) 4516-25.

[116]   Im H and Kim J 2012 Thermal conductivity of a graphene oxide-carbon nanotube hybrid/epoxy composite *Carbon* **50**(15) 5429-40.

46

[117]   Sun Y, Tang B, Huang W, Wang S, Wang Z, Wang X, Zhu Y and Tao C 2016 Preparation of graphene modified epoxy resin with high thermal conductivity by optimizing the morphology of filler *Appl. Therm. Eng*. **103** 892-900.

[118]   Bryning M B, Milkie D E, Kikkawa J M and Yodh A G 2005 Thermal conductivity and interfacial resistance in single-wall carbon nanotube epoxy composites *Appl. Phys. Lett*. **87**(16) 161909-1-3.

[119]   Huxtable S T *et al.* 2003 Interfacial heat flow in carbon nanotube suspensions *Nat. Mater*. **2**(11) 731-4.

[120]   Yan H, Wang R, Li Y and Long W 2014 Thermal Conductivity of Magnetically Aligned Graphene Polymer Composites with Fe_3O_4-Decorated Graphene Nano-sheets *J. Electron. Mater*. **44**(2) 658-66.

[121]   Luo F, Wu K, Guo H, Zhao Q and Lu M 2016 Anisotropic thermal conductivity and flame retardancy of nanocomposite based on mesogenic epoxy and reduced graphene oxide bulk *Compos.Sci.Technol.***132** 1-8

[122]   Mahanta N K, Loos M R, Zlocozower I M and Abramson A R 2015 Graphite-graphene hybrid filler system for high thermal conductivity of epoxy composites *J. Mater. Res*. **30**(7) 959-66.

[123]   Berber S, Kwon Y K and Tomn D 2000 Unusually high thermal conductivity of carbon nanotubes *Phys. Rev. Lett*. **84**(20) 4613.

[124]   Hone J, Whitney M and Zettl A 1999 Thermal conductivity of single-walled carbon nanotubes *Phys. Rev. B* **59**(4) R2514.

[125]   Biercuk M, Llaguno M C, Radosavljevic M, Hyun J K and Johnson A T 2002 Carbon nanotube composites for thermal management *Appl. Phys. Lett*. **80**(15) 2767-69.

[126]   Yu A, Ramesh P, Sun X, Bekyarova E, Itkis M and Haddon R 2008 Enhanced thermal conductivity in a hybrid graphite nanoplatelet - Carbon nanotube filler for epoxy composites *Adv. Mate*r. **20**(24) 4740-44.

[127]   Yang S, Lin W, Huang Y and Wang Y 2011 Synergetic effects of graphene platelets and carbon nanotubes on the mechanical and thermal properties of epoxy composites *Carbon* **49**(3) 793-803.

[128]   Yu L, Park J S, Lim Y S, Lee C S, Shin K, Moon H J, Yang C M, Lee Y S and Han J H 2013 Carbon hybrid fillers composed of carbon nanotubes directly grown on graphene nano-platelets for effective thermal conductivity in epoxy composites *Nanotechnology* **24**(15) 1-10.

[129]   Messina E *et al*. 2016 Double-Wall nanotubes and graphene nanoplatelets for hybrid conductive adhesives with enhanced thermal and electrical conductivity *ACS Appl. Mater. Interfaces* **8** 23244−59.

[130]   Zha J, Zhu T, Wu Y, Wang S, Li R and Dang Z 2015 Tuning of thermal and dielectric properties for epoxy composites filled with electrospun alumina fibers and graphene nano-platelets through hybridization *J. Mater. Chem. C* **3**(27) 7195-202.

[131]   Yuan W, Xiao Q, Li L and Xu T 2016 Thermal conductivity of epoxy adhesive enhanced by hybrid graphene oxide/AlN particle *Appl. Therm. Eng*. **106** 1067-74.

[132]   Gao Z and Zhao L 2015 Effect of nano-fillers on the thermal conductivity of epoxy composites with micro-Al_2O_3 particles *Mater. Des*. **66** 176-82.

[133]   Wang Y, Yu J, Dai W, Wang D, Song Y, Bai H, Zhou X, Li C, Lin C and Jiang N 2014 Epoxy composites filled with one-dimensional SiC nanowires-two-dimensional graphene nano-platelets hybrid nanofillers. *RSC Adv.* **4**(103) 59409-17.

48